Report to the Norwegian Directorate of Fisheries

The role and range boundaries of gelatinous zooplankton in the rapidly changing Arctic marginal seas

Cruise No. HE605

RISING

Role and Distribution of Jellies in Norwegian waters

Norwegian Licence No. 819/2022
08.02.2022, 09.08.2022-04.09.2022, Jnr. 22/2153
NPD 2022/321/KK
Research in Svalbard RIS ID 11915

Dr. Charlotte Havermans
Alfred Wegener Institute Helmholtz Centre for Polar and Marine Research

2022

Table of Contents

1 Cruise Summary

1.1 Summary in English

The HE605 expedition with R/V Heincke aimed to characterize zooplankton communities in fjords and open ocean, along a poleward latitudinal gradient, from Northern Norway to Svalbard. The focus of the cruise was the study of gelatinous zooplankton (cnidarian medusae, ctenophores and pelagic tunicates), investigating their species diversity, distribution patterns, ecological role and adaptation potential. By comparing Arctic and Atlantic fjords influenced by distinct water regimes, the obtained data will lay a solid baseline of gelatinous zooplankton diversity and distributions. Comparing Arctic vs. Atlantic community compositions will allow us to better predict climate-change driven poleward range shifts of Atlantic species under ongoing environmental changes.

The expedition started on the 9th of August, sailing to Svalbard during a 6-day transit to Krossfjorden, where scientific station worked started on the 15th of August in the morning. We visited five western Svalbard fjords, of which the degree of Atlantic influence differs: Krossfjorden, Kongsfjorden, Billefjorden, van Mijenfjorden and Hornsund. On the way south to mainland Norway, we sampled at three localities in the open Barents Sea. Thereafter, we sampled in various localities in Porsangerfjorden, northern Norway, and on the borders of the Bleik Canyon near Andøya. Scientific deployments included the CTD/rosette water sampler to measure physical properties of the water column and sample water for environmental (eDNA analyses), the Van Veen Grab to collect sediment for eDNA analyses, plankton nets to collect zooplankton and small nekton (Bongo, WP3 and Multi-nets), scientific angling for fish, and optical video platforms including the Pelagic In-situ Observation System PELAGIOS, the Ocean Floor Observation System OFOS and a BlueROV2. During the expedition, more than 2000 zooplankton samples were collected for morphological, molecular, biomarker and contaminant analyses, 114 sediment samples and 518 filters for eDNA analyses, and over 14 hours of video footage was recorded for in-situ observations of gelatinous and other organisms. These samples and data will be used for different projects under the umbrella of the Helmholtz Young Investigator Group ARJEL at the AWI, and ongoing research projects at GEOMAR and the University of Bergen.

1.2 Zusammenfassung

Die Expedition HE605 mit der R/V Heincke hatte zum Ziel, die Zooplanktongemeinschaften in Fjorden und im offenen Ozean entlang eines polwärts gerichteten Breitengrades von Nordnorwegen bis Spitzbergen zu charakterisieren. Der Schwerpunkt der Reise lag auf der Untersuchung von gelatinösem Zooplankton (Nesseltiere, Ctenophoren und pelagische Manteltiere), wobei Artenvielfalt, Verteilungsmuster, ökologische Rolle und Anpassungspotenzial untersucht wurden. Durch den Vergleich arktischer und atlantischer Fjorde, die von unterschiedlichen Wasserregimen beeinflusst werden, werden die gewonnenen Daten eine solide Grundlage für die Vielfalt und Verteilung des gelatinösen Zooplanktons bilden. Der Vergleich der Zusammensetzung der arktischen und atlantischen planktongemeinschaften wird

es uns ermöglichen, die durch den Klimawandel bedingten Verschiebungen der Verbreitungsgebiete atlantischer Arten nach Norden besser vorherzusagen.

Die Expedition begann am 9. August mit der Überfahrt nach Svalbard und einem 6-tägigen Transit zum Krossfjorden, wo am 15. August morgens die wissenschaftliche Arbeit begann. Wir besuchten fünf Fjorde in Westsvalbard, die sich im Umfang der atlantischen Gewässer unterscheiden: Krossfjord, Kongsfjord, Billefjord, van Mijenfjord und Hornsund. Auf dem Weg nach Süden zum norwegischen Festland haben wir an drei Orten in der Barentssee Proben genommen. Danach beprobten wir verschiedene Orte im Porsangerfjord, Nordnorwegen, und in dem Bleik-Canyon bei Andøya. Zu den wissenschaftlichen Einsätzen gehörten der CTD/Rosette zur Messung der physikalischen Eigenschaften der Wassersäule und zur Entnahme von Wasserproben für Umwelt-DNA Analysen (eDNA), der Van-Veen-Greifer zur Entnahme von Sediment für eDNA-Analysen, Planktonnetze zur Entnahme von Zooplankton (Bongo-, WP3- und Multinetze), wissenschaftliches Angeln nach Fischen und optische Videoplattformen wie das „Pelagic In-situ Observation System“ (PELAGIOS), das „Ocean Floor Observation System“ (OFOS) und ein ROV (BlueROV2). Während der Expedition wurden mehr als 2000 Zooplanktonproben für morphologische, molekulare, Biomarker- und Schadstoffanalysen, 114 Sedimentproben und 518 Filter für eDNA-Analysen entnommen und über 14 Stunden Videomaterial für In-situ-Beobachtungen von gelatinösen und anderen Organismen aufgezeichnet. Diese Proben und Daten werden für verschiedene Projekte der Helmholtz-Nachwuchsgruppe ARJEL am AWI sowie für laufende Forschungsprojekte am GEOMAR und an der Universität Bergen verwendet.

2 Participants

2.1 Principal Investigators

Name	Institution
Havermans, Charlotte, Dr.	AWI

2.2 Scientific Party

Name	Discipline	Institution
Havermans, Charlotte, Dr.	Marine Ecology / Chief Scientist	AWI
Dischereit, Annkathrin	Marine Ecology / Doctoral Researcher	AWI
Eschbach, Andrea	Molecular Ecology / Technical Assistant	AWI
Hampe, Hendrik	Marine Technology / Technical Assistant	GEOMAR
Hosia, Aino, Prof. Dr.	Marine Ecology / Professor	UiB
Rathnayake, Ishani	Marine Ecology / MSc student	AWI
Soto-Angel, Joan, Dr.	Marine Ecology / Scientist	UiB
Stenvers, Vanessa	Marine Ecology / Doctoral Researcher	GEOMAR
Steiner, Niko	Marine Ecology / MSc student	AWI
Stoltenberg, Ina	Marine Ecology / Doctoral Researcher	GEOMAR
Throm, Julia	Marine Ecology / MSc student	AWI

2.3 Participating Institutions

AWI	Alfred-Wegener-Institut Helmholtz-Zentrum für Polar- und Meeresforschung
GEOMAR	Helmholtz-Zentrum für Ozeanforschung Kiel
UiB	University Museum of Bergen, University of Bergen

3 Research Program

3.1 Description of the Work Area

Svalbard fjords are influenced by both Atlantic and Arctic water masses, in addition to locally formed water masses (Cottier et al. 2005; Hop et al. 2019). The West Spitsbergen Current (WSC), flowing along the west coast of Svalbard, brings in warm and salty Atlantic water into the Arctic, whereas the polar-influenced Svalbard Coastal Current moves northward, closer to the coast, along western Svalbard (Sternal et al. 2014). Mixing of these two currents results in the formation of transformed Atlantic water, which expands across the shelf and penetrates the fjords (Nilsen et al. 2016). Indeed, this Atlantic water enters the western Svalbard fjords as bottom currents, below the Arctic water, mixes with fresher water in the fjords and returns as surface currents (Mangerud & Svendsen 2018).

The environmental characteristics of the different fjord systems are influenced by the relative influence of these two water masses, as well as by sea-ice processes and marine terminating glaciers more inwards into the fjord (Cottier et al. 2010). The inflow of Atlantic water also depends on the extent and depth of the sill of the respective fjord, acting as a barrier for the inflow of warm saline Atlantic water, which is denser, and therefore situated deeper, than the local cold and fresh glacial meltwater outflow. In general, Svalbard fjord systems are characterized by strong environmental gradients and are partially covered with sea ice in winter. The outer fjords are mainly influenced by the influx of the oceanic water masses (WSC and fresh and cold coastal currents), whereas the inner fjords are strongly influenced by retreating tidewater glaciers and meltwater discharge, creating small-scale variations in salinity, temperature, nutrients and organic matter (Węsławski et al. 1995; Nilsen et al. 2008).

During the HE605 expedition, we visited five Svalbard fjords. These are all situated along the "Atlantic highway" into the Arctic Ocean, but their level of Atlantic influence differs. The Kongsfjorden-Krossfjorden system is largely dominated by warm water masses from the WSC, whereas Billefjorden and Hornsund are predominantly influenced by Arctic water masses (Cottier et al. 2005; Cisek et al. 2017). The five fjords significantly differ in salinity, water temperature, freshwater input, nutrient supply and phyto- and zooplankton community dynamics (Walkusz et al. 2003; Cottier et al. 2010; Prominska et al. 2017; Bae et al. 2022).

The two fjords **Kongsfjorden** and **Krossfjorden** system are connected through a common mouth, with a trench of decreasing depth towards the shallow shelf. Exchanges between the shelf and fjord bring in warmer WSC and colder Arctic waters. Kongsfjorden is oriented from southeast to northwest, and Krossfjorden from north to south. Kongsfjorden is 20km long, and has an inner fjord with shallow water less than 100m, whereas its deeper fjord reaches depths below 300m. Krossfjorden is about 30km long, and consists of two inner parts (Svendsen et al. 2002). Both fjords are strongly influenced by the presence of tidewater glaciers, one at the head of Krossfjorden, five calving glaciers along the eastern coast of Kongsfjorden and two on its northern coast (Svendsen et al. 2002).

Billefjorden is a sill fjord that opens composed of an outer basin (max. depth of ca. 230m), isolated from Isfjorden by a ca. 80m sill, and an inner basin (max. depth of ca. 190m). A large glacier, at the head of the fjord, supplies the fjord with meltwater and sediment in summer and autumn (Arnkvaern et al. 2005).
Van Mijenfjorden is another glacially influenced fjord, albeit less glaciated than Kongsfjorden. Landfast ice forms in winter due to the island Akseløya, closing off the fjord almost entirely at its mouth. It is 60km long and consists of two basins, one deep basin (max. depth 115m), separated from a shallower, inner basin (max. depth of 74m) by a 45m sill (Fer & Widell 2007; Skarðhamar & Svendsen 2010). The fjord is influenced by Atlantic waters of the WSC, albeit to a lesser extent as the Kongsfjorden-Krossfjorden system due to the narrow sounds at either side of the island, limiting water exchange. In addition to several rivers discharging into the fjord, bringing in freshwater, two glaciers calve into the fjord. Due to these characteristics and its semi-enclosed nature, it is highly influenced by local physical processes, landfast ice, and local water masses (e.g., Winter Cooled water masses) (Skarðhamar & Svendsen, 2010).
Hornsund is the southernmost fjord on the Svalbard's west coast, it is 34km long, connected to the open sea through a wide opening (Blaszczyk et al. 2013). It has no sill at the entrance, facilitating the penetration of WSC at depth as well as colder waters at the surface. It is influenced by warm (WSC) and the coastal cold currents. The fjord is influenced by fourteen tidewater glaciers, which strongly modify the physical environment with massive meltwater outflow resulting in stratification and little vertical exchange (Swerpel 1985).
Over recent decades, **Svalbard fjords** have undergone major physical and biotic changes due to climate change. Glacier melting results enhances freshwater plumes and turbidity, altering the hydrographic environment and light regime (van de Poll et al. 2018). This, together with warming waters, impacts primary producer communities (e.g., Neukermans et al. 2018; Payne & Roesler 2019), which is eventually translated to higher trophic levels. Zooplankton communities have also seen new species shifting in from warmer waters further south, due to increased water temperatures in several Svalbard fjords (e.g., Buchholz et al. 2010; Geoffroy et al. 2018).

The **Barents Sea** is an Arctic inflow shelf, receiving large inputs of Atlantic water (Carmack & Wassmann 2006; Jakobsen & Ozhigin 2011). The Polar Front is a boundary zone located in the Barents Sea, where the Atlantic water flowing north and eastward eventually meets colder and fresher Arctic Water flowing south (Oziel et al. 2016). The Atlantic water typically cools and mixes with other water masses in the area, forming Barents Sea Water, penetrating under the Arctic water north of the Polar Front (Lind et al. 2012; Oziel et al. 2016; Descôteaux et al. 2021). This Atlantic water can entrain high abundances of organisms onto the Arctic shelf. This includes zooplankton species, or meroplanktonic larvae of benthic species, with a boreal-Atlantic origin. With further climate warming, the Barents Sea is likely to receive increasing numbers of boreal species extending their range into the Arctic (Renaud et al. 2015, Descôteaux et al. 2021), hence, monitoring Barents Sea communities can be crucial for detecting range shifts.

Porsangerfjorden is the largest fjord in northern Norway (Svendsen 1991), covering an area of 1800 km^2, and facing the Barents Sea towards the north. A sill of 60m separates the fjord into an outer and inner basin (Eilertsen & Frantzen 2007). The outer basin, with a maximum depth of 285m, and 300m depth at its mouth, is characterized by a frequent exchange of deepwater with the Norwegian Coastal Current, and hence considered an extension of the coastal zone

(Wassmann et al. 1996; Källgren et al. 2015). The inner area, consisting of two deep basins at ca. 100m depth, is characterized by locally formed Arctic waters. These cold waters, lingering below the thermocline in the deep basins, cause bottom temperatures to remain around zero degrees throughout the year. The inner area also receives a significant input of freshwater from river runoffs, resulting in a decreasing salinity gradient from the outer to the inner area. The inner area possesses a diverse Arctic fauna and is therefore considered an isolated Arctic environment on mainland Norway (Svendsen 1991; Christiansen & Fevolden 2000).

The **Bleik Canyon** is situated offshore from the island Andøya, located in Vesterålen, northern Norway. It is about 40-50km long and has a maximum width of 20km. At its mouth, it reaches a maximum depth of about 3000m (Laberg et al. 1999; 2007). It is characterized by steep sides of complex topography, inducing upwelling in the coastal current (Blindheim 1985). This upwelling renders the area highly productive, attracting large fish, cephalopods, seabirds and marine mammals such as sperm whales (Skjoldal 2004; Rødland & Bjørge 2015). It remains however understudied with regarded to the zooplankton communities inhabiting this area.

3.2 Aims of the Cruise

The overarching goals of this expedition, covering a poleward gradient (Svalbard, Barents Sea, Northern Norway), were to obtain a baseline of gelatinous zooplankton (GZP) diversity, abundance and distribution and link these to distinct local water masses.
We applied an integrative survey combining plankton net catches with modern technologies in optics together with state-of-the-art molecular analyses to realize the following objectives:

- Obtain species inventories and abundances of GZP and other plankton/nekton species. This is achieved along a latitudinal gradient, and in fjords with a different degree of Atlantic vs. Arctic water mass influence, as well as along a vertical (depth) gradient;
- Reveal the molecular diversity of species encountered in different water masses, regions and depths and evaluate the genetic connectivity between regional populations of dominant species;
- Characterize local species boundaries across environmental gradients (Atlantic vs Arctic water masses, surface to deep) of GZP to better understand their habitat preference, eventually feeding these data into modelling efforts;
- Identify the efficiency of environmental DNA (eDNA) to characterize zooplankton communities over spatial and temporal scales;
- Elucidate the tropic role of GZP in regional food webs, as predator, and as prey for fish species;
- Evaluate the importance of jellyfish carcasses as vectors for carbon, linking pelagic and benthic food webs;
- Assess the role of jellyfish and other zooplankton as vectors for microplastics and, potentially, other contaminants;
- Investigate the occurrence of parasitism in (semi)-GZP such as scyphozoans, hydrozoans, and chaetognaths;
- Evaluate the response of dominant zooplankton to stressors.

3.3 Agenda of the Cruise

After a transit from Bremerhaven to Svalbard, station work was initiated in Krossfjorden. Sampling was planned at three different stations/localities in each of the five different Svalbard fjords, from North to South: Krossfjorden, Kongsfjorden, Billefjorden, Van Mijenfjorden, Hornsund. After this, the Barents Sea crossing started, and sampling was carried out at three stations in the southern Barents Sea. The next working area was Porsangerfjorden, with three major sites in the outer basin, one site near the sill separating inner and outer area, and one site in the inner basin. Finally, after steaming to the Vesterålen area, station work was carried out on the border of the Bleik canyon near Andøya, at three stations situated at ca. 300, 600 and 1200m of depth.

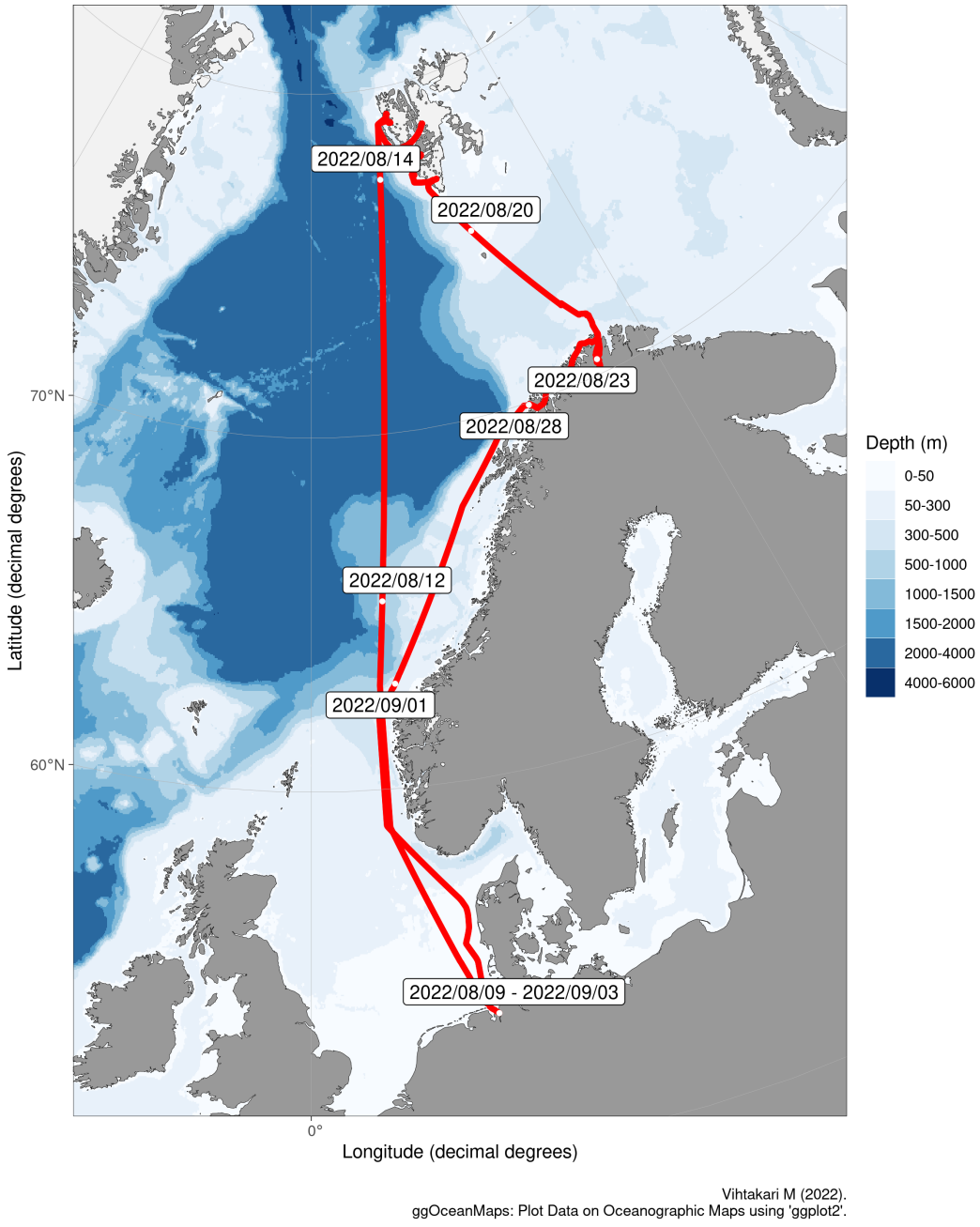

Fig. 3.1 Track chart of R/V HEINCKE Cruise HE605 with the cruise track to the main working areas: West Svalbard, Barents Sea, Porsangerfjorden and the Bleik Canyon (www.pangaea.de).

4 Narrative of the Cruise

We boarded the ship on the 8th of August in the morning, after having received the results of our negative COVID19 PCR tests. That day, we unpacked and set up the labs after which we spent one night in the harbor. On the 9th of August, we left port around 8am in Bremerhaven and set sail for the Arctic under a blue sky and calm sea. We spent the transit time to unpack and set up our gear, have scientific talks and plan our station work in further detail. On the 12th of August, before noon, we crossed the polar circle. On the way northward, we had around 1m swell and 4-6 Bft winds. On the 15th of August, shortly before 10am, we started first station work in Krossfjorden, where we sampled at three different stations until late afternoon. We deployed CTD, grab, Multinet, Bongonet and the PELAGIOS towed camera system. Then we steamed to Kongsfjorden. On the 16th, we had further station work in Kongsfjorden. Some brash ice was observed in the fjord, therefore the stations nearer to the glacier could not be sampled as planned. We were nevertheless able to deploy the CTD rosette, grab, WP3 net and PELAGIOS. At 2pm, Heincke laid at the pier of Ny-Ålesund, where we received frozen freight from the AWIPEV station to store in the ship's freezers and cold room, and bring it back to Bremerhaven. At 4pm, we started steaming towards Billefjorden. On the way, at the mouth of Kongsfjorden, we had a station for scientific angling. On the 17th of August, we reached Billefjorden, and sampling started at 8am. Here, we deployed the CTD rosette, grab, nets at three stations, as well as the OFOS bottom camera for the first time. On the 18th, we reached Van Mijenfjorden, started station work from ca. 8am to 3pm. We deployed CTD rosette, grab, WP3, Multinet, Bongonet at three different stations and also carried out an OFOS transect. We left the fjord soon after 3pm, but encountered strong swell (5m) once outside the fjord, in the evening. This lasted for the entire night, during which the ship could not make much progress and then positioned itself to wait for the storm to pass. We only entered Hornsund around 2pm in the afternoon of the 19th of August, where sampling started at 4pm. There was still a swell of 3m inside the fjord. We deployed CTD rosette, grab, all plankton nets and also had an OFOS and PELAGIOS survey. After station work was done, we started steaming, heading for the Norwegian mainland. During the crossing of the Barents Sea, we carried out a scientific angling station on the Spitsbergen Bank, with a low swell (0-1m) and foggy sky. We sampled the first Barents Sea station on the 21st of August, around 8am. We deployed the CTD rosette, grab, all plankton nets and also had a PELAGIOS survey. We reached Barents Sea station 2 shortly after 3pm, and the third open-water station in the evening at 6pm. Here, we carried out CTD rosette, grab and net deployments. After that, we entered Porsangerfjorden, where we started station work on the 22nd of August at 8am. At this station, situated midway across the length of the fjord, we deployed six CTD rosette in a row, followed by a grab and all different net deployments. The zodiac was used for a deployment of the BlueROV2 by two scientific crew. In the evening, a station for scientific angling was carried out. Winds increased over the next hours, up to 8-9 Bft on the 23rd of August. Hence, we needed to shelter until the next morning, when we were able to resume station work. We deployed the CTD rosette, had multiple grab deployments followed by net catches with all different nets, and surveys with OFOS and PELAGIOS. We celebrated having past half of the cruise with a Bergfest in the evening. The weather was nice, a blue sky and a nice view over the hills surrounding Porsangerfjorden. On the 25th, we sampled with the CTD rosette, the grab, plankton nets, OFOS and PELAGIOS. We also carried out a sample handover from the Porsanger field station (Institute of Marine Research) Børselv, of samples being collected by

colleagues from Uni Bremen and AWI earlier this summer. In the evening, we had another scientific angling station. The 26th of August was our last day in Porsangerfjorden. We sampled in stations further north in the fjord, one where we did, besides CTD rosette, grab and net deployments, also an OFOS transect. At the last station at the mouth of the fjord, characterized by an Atlantic water regime, we deployed the CTD rosette, grab, and plankton nets. In the evening, we had another but not very successful angling station. Around 7:30pm, we started steaming towards the Vesterålen area. On the 27th, we were steaming through the fjord, under a thick cloud over. Winds increased and on the 28th of August, we spent some time sheltering, as winds were up to 6-7 Bft. On the 29th, we resumed station work at 4 Bft and 1.5m swell. We carried out two stations at the Bleik Canyon, one where the water depth was about 600m, and the second one with almost 1300m water depth. Two CTDs were carried out at each of these stations, followed by grab (unsuccessful), and plankton nets. On the 30th of August, we had our last day of sampling. We carried out station work at the border of the canyon (ca. 300m depth), and had deployments of the CTD rosette and three nets. At 11:30 am, station work ended. During the expedition, more than 2000 zooplankton samples were collected for morphological, molecular, biomarker and contaminant analyses, 114 sediment samples and 518 filters for eDNA analyses, and over 14 hours of video footage was recorded from water column and seafloor surveys. The transect to Bremerhaven was rather calm, with 1-1.5m swell. We arrived in the evening of the 3rd of September in Bremerhaven, under a same blue sky as when we left, four weeks earlier. Most of the scientific crew left the ship around 9pm, while some others stayed overnight and left in the early morning of the 4th. In total, the cruise covered 4070 nautical miles.

5 Preliminary Results (work at sea)

5.1 CTD Measurements and Sampling for environmental DNA with the Rosette

(A. Eschbach[1], C. Havermans[1], A. Dischereit[1], N. Steiner[1])

[1]AWI

At each station, one or more CTD casts preceded the sediment and zooplankton sampling. The CTD (SBE 49, Sea-Bird Scientific) was operated on board by Andrea Eschbach and Niko Steiner. Depth distribution of water masses was determined based on the vertical profiles of temperature, salinity and fluorescence measurements (as a proxy for chlorophyll a concentration). Data were processed on the ManageCTD software and transformed to be displayed in Ocean Data View (https://odv.awi.de). For this, only the downcast was considered; the beginning of each cast, when pumps are not yet switched on, was removed from the profile and the profile was de-spiked.

For environmental DNA (eDNA) analyses, water samples were collected at all CTD stations, using the rosette water sampler, collecting water at 5 to 6 different depths from above the seafloor to the surface (depending on the local water depth at the station; see Table 1). At station 21 (POR-1), several CTD/rosette casts were carried out one after the other, in order to assess short-term temporal variation in zooplankton communities detected with eDNA at one sampling point (see chapter 5.2). Two bottles were capped at each depth. 6 L of water per depth were collected in a canister and filtered through 0.22 µm Sterivex Millipore filters (Polyethersulfone Membrane Filters) in triplicates of two liters per filter. A control filtration of 2 L Milli Q Water per station was performed at the beginning of the filtration process. After each station, the canisters were cleaned with 1:10 diluted bleach and rinsed with MilliQ Water. The filters were

stored on ice and then frozen at -80 °C until DNA extraction will be performed in the AWI laboratories.

Table 1 Rosette sampling details (coordinates, bottom depth, sampling depths) for environmental DNA analyses at each of the stations. The following abbreviations are used for the station localities: KROSS = Krossfjorden, KONG = Kongsfjorden, BIL = Billefjorden, VMF = Van Mijenfjorden, HORN = Hornsund, BAR = Barents Sea, POR = Porsangerfjorden, BLC = Bleik Canyon (Vesterålen).

Station No.		Date	Gear	Latitude	Longitude	Water Depth	Remarks/Recovery
HEINCKE	AWI	2022		[°N]	[°E]	[m]	Sampled depths for eDNA
HE605_1-1	KROSS-1	15.8	ROS/CTD	79° 11,755'	011° 47,602'	365	340, 201, 100, 50, 20, 2.5m
HE605_2-1	KROSS-2	15.8.	ROS/CTD	79° 07,751'	011° 40,583'	329	309, 200, 100, 50, 20, 2m
HE605_3-1	KONG-1	15.8	ROS/CTD	78° 58,358'	011° 46,461'	221	209, 100, 70, 50, 20, 2.5m
HE605_5-1	KONG-3	16.8	ROS/CTD	78° 56,782'	011° 55,100'	292	265, 200, 100, 50, 20, 2m
HE605_7-1	BIL-1	17.8	ROS/CTD	78° 39,698'	016° 43,890'	192	170, 100, 70, 50, 20, 2m
HE605_8-1	BIL-2	17.8	ROS/CTD	78° 39,555'	016° 40,611'	190	170, 100, 70, 50, 20, 2m
HE605_9-1	BIL-3	17.8	ROS/CTD	78° 37,562'	016° 33,256'	140	115, 100, 70, 50, 20, 3.5m
HE605_10-1	VMF-1	18.8	ROS/CTD	77° 45,773'	015° 08,472'	105	90, 70, 50, 20, 2m
HE605_11-1	VMF-2	18.8	ROS/CTD	77° 47,956'	015° 19,809'	104	90, 70, 50, 20, 2m
HE605_12-1	VMF-3	18.8	ROS/CTD	77° 46,179'	015° 16,764'	101	85, 70, 50, 20, 2.5m
HE605_13-1	HORN-1	19.8	ROS/CTD	76° 59,806'	016° 26,708'	125	111, 70, 50, 20, 2m
HE605_14-1	HORN-2	19.8	ROS/CTD	76° 59,519'	016° 00,681'	107	95, 70, 50, 20, 2m
HE605_15-1	HORN-3	19.8	ROS/CTD	76° 57,742'	015° 49,667'	223	205, 100, 50, 20, 2m
HE605_18-1	BAR-1	21.8	ROS/CTD	72° 16,771'	024° 26,181'	268	250, 201, 100, 50, 20, 3.5m
HE605_19-2	BAR-2	21.8	ROS/CTD	71° 48,735'	025° 34,401'	282	260, 201, 100, 50, 20, 2m
HE605_20-1	BAR-3	21.8	ROS/CTD	71° 41,652'	026° 12,151'	326	310, 200, 100, 51, 21, 2m
HE605_21-1	POR-1	22.8	ROS/CTD	70° 31,774'	025° 39,012'	152	135, 100, 70, 50, 2m
HE605_21-2	POR-1	22.8	ROS/CTD	70° 31,761'	025° 39,057'	150	135, 100, 70, 50, 2m
HE605_21-3	POR-1	22.8	ROS/CTD	70° 31,772'	025° 39,081'	150	135, 100, 70, 50, 2m
HE605_21-4	POR-1	22.8	ROS/CTD	70° 31,746'	025° 39,154'	148	135, 100, 70, 50, 3m
HE605_21-5	POR-1	22.8	ROS/CTD	70° 31,731'	025° 38,949'	152	135, 100, 70, 50, 2m
HE605_21-6	POR-1	22.8	ROS/CTD	70° 31,714'	025° 39,067'	148	135, 100, 70, 50, 2m
HE605_23-1	POR-3	24.8	ROS/CTD	70° 05,294'	025° 06,593'	78	65, 50, 20, 10, 2m
HE605_24-1	POR-4	25.8	ROS/CTD	70° 18,584'	025° 18,021'	87	75, 50, 20, 10, 2m
HE605_26-1	POR-6	26-1	ROS/CTD	70° 53,197'	026° 03,939'	194	179, 100, 71, 51, 21, 2.5m
HE605_27-1	POR-7	27-1	ROS/CTD	71° 05,466'	026° 19,723'	165	149, 100, 70, 50, 20, 2m
HE605_29_1	BLC-1	29-1	ROS/CTD	69° 30,355'	015° 45,680'	631	300, 200, 100, 50, 20, 2m
HE605_29_2	BLC-1	29-2	ROS/CTD	69° 30,356'	015° 45,653'	637	600. 500. 400, 300m
HE605_30_1	BLC-2	30-1	ROS/CTD	69° 28,008'	015° 39,007'	1112	400, 300, 200, 100, 50, 2m
HE605_30_2	BLC-2	30-2	ROS/CTD	69° 28,029'	015° 39,011'	1279	1240, 1200, 1100, 900, 700, 500m
HE605_31_1	BLC-3	31-1	ROS/CTD	69° 29,737'	015° 47,560'	314	Water sampling failed

5.2 Sampling with plankton nets and zooplankton sorting

(A. Hosia[1], J.J. Soto-Angel[1], A. Dischereit[2], J. Throm[2], I. Stoltenberg[3], V. Stenvers[3], C. Havermans[2], H. Hampe[3])

[1]UiB

[2]AWI

[3]GEOMAR

Zooplankton samples for species identification, abundance data, molecular analyses and experimental work were collected using Midi-Multinet, WP3 and Bongo net deployments (Table 2). The Midi-Multinet (mesh sizes 330 µm) were deployed vertically through the water column at a speed of 0.5 m/s with five different opening and closing nets for depth-stratified sampling. The Bongo net (mesh size 500 µm) was equipped with a large non-filtering cod-end and a V-Fin depressor. It was towed obliquely at a ship's speed of 1.5-2 knots and a wire speed of 0.3-0.5

m/s. The WP3 had a large closed cod-end and mesh size of 1000 µm. For sampling the fragile GZP, the WP3 net was lowered at 0.5 m/s but hauled at 0.2 m/s. The nets were equipped with flowmeters for obtaining abundance values, and a depth logger and CTD for obtaining in-situ measurements of environmental conditions and the maximum depth reached.

Table 2 Net sampling details (coordinates, bottom depth, sampling depths) at each of the stations. The following abbreviations are used for the station localities: KROSS = Krossfjorden, KONG = Kongsfjorden, BIL = Billefjorden, VMF = Van Mijenfjorden, HORN = Hornsund, BAR = Barents Sea, POR = Porsangerfjorden, BLC = Bleik Canyon (Vesterålen).

Station No.		Date	Gear	Latitude	Longitude	Water Depth	Remarks/Recovery
HEINCKE	AWI	2022		[°N]	[°E]	[m]	
HE605_1-3	KROSS-1	15.8	Multi-net	79° 11,152'	011° 47,495'	363	300-200, 200-100, 100-50, 50-20, 20-0m
HE605_1-4	KROSS-1	15.8.	Bongo	79° 11,027'	011° 47,888'	362	Wire length 450m
HE605_2-3	KROSS-2	15.8	Multi-net	79° 07,234'	011° 39,078'	326	310-200, 200-100, 100-50, 50-20, 20-0m
HE605_3-3	KONG-1	15.8	WP3	78° 58,499'	011° 46,020'	188	Wire length 178m
HE605_3-4	KONG-1	15.8	Bongo	78° 58,719'	011° 41,419'	326	312m depth on pressure sensor
HE605_3-5	KONG-1	15.8	Bongo	78° 58,726'	011° 42,470'	312	267m depth on pressure sensor
HE605_3-6	KONG-1	15.8	Multi-net	78° 58,802'	011° 39,034'	307	210-100, 100-70, 70-50, 50-20, 20-0m
HE605_5-3	KONG-3	16.8	WP3	78° 56,801'	011° 54,940'	284	Wire length 260m
HE605_5-4	KONG-3	16.8	WP3	78° 56,794'	011° 54,806'	272	Wire length 240m
HE605_5-6	KONG-4	16.8	WP3	78° 56,781'	011° 55,308'	297	Wire length 269m
HE605_7-3	BIL-1	17.8	WP3	78° 39,858'	016° 43,725'	191	Wire length 170m
HE605_7-4	BIL-1	17.8	WP3	78° 39,947'	016° 43,431'	184	Wire length 164m
HE605_7-5	BIL-1	17.8	Multi-net	78° 39,198'	016° 40,303'	200	160-100, 100-70, 70-50, 50-20, 20-0m
HE605_8-3	BIL-2	17.8	WP3	78° 39,618'	016° 40,875'	191	Wire length 170m
HE605_8-4	BIL-2	17.8	Multi-net	78° 39,102'	016° 38,975'	174	150-100, 100-70, 70-50, 50-20, 20-0m
HE605_9-3(-1)	BIL-3	17.8	WP3	78° 37,755'	016° 33,844'	134	Wire length 115m
HE605_9-3(-2)	BIL-3	17.8	WP3	78° 37,590'	016° 33,379'	137	Wire length 117m
HE605_9-4	BIL-3	17.8	Multi-net	78° 37,850'	016° 33,526'	147	115-100, 100-70, 70-50, 50-20, 20-0m
HE605_10-5	VMF-1	18.8	WP3	77° 45,771'	015° 08,435'	105	Wire length 85m
HE605_10-6	VMF-1	18.8	Multi-net	77° 46,124'	015° 08,240'	104	91-70, 70-50, 50-20, 20-0m
HE605_10-7	VMF-1	18.8	Bongo	77° 46,034'	015° 09,567'	104	80m depth on pressure sensor
HE605_11-3	VMF-2	18.8	WP3	77° 47,936'	015° 20,878'	105	Wire length 85m
HE605_11-4	VMF-2	18.8	Multi-net	77° 48,297'	015° 19,126'	103	90-70, 70-50, 50-20, 20-0m
HE605_12-3	VMF-3	18.8	WP3	77° 46,127'	015° 17,179'	100	Wire length 80m
HE605_12-4	VMF-3	18.8	Multi-net	77° 46,710'	015° 16,601'	106	90-70, 70-50, 50-20, 20-0m
HE605_13-5	HORN-1	19.8	WP3	76° 59,749'	016° 26,942'	124	Wire length 110m
HE605_13-6	HORN-1	19.8	Multi-net	76° 59,664'	016° 25,976'	127	115-100, 100-70, 70-50, 50-20, 20-0m
HE605_13-7	HORN-1	19.8	Bongo	76° 59,678'	016° 26,878'	124	Wire length 164m
HE605_14-3	HORN-2	19.8	Multi-net	76° 59,332'	015° 59,994'	113	96-70, 70-50, 50-20, 20-0m
HE605_15-3	HORN-3	19.8	WP3	76° 57,730'	015° 49,557'	223	Wire length 200m
HE605_15-4	HORN-3	19.8	Multi-net	76° 58,063'	015° 50,709'	211	200-100, 100-70, 70-50, 50-20, 20-0m
HE605_18-3	BAR-1	21.8	WP3	72° 16,795'	024° 26,123'	250	Wire length 269m
HE605_18-4	BAR-1	21.8	Multi-net	72° 17,390'	024° 26,728'	266	250-200, 200-100, 100-50, 50-20, 20-0m
HE605_18-6	BAR-1	21.8	Bongo	72° 19,395'	024° 29,092'	266	Wire length 337m
HE605_19-4	BAR-2	21.8	Multi-net	71° 49,013'	025° 36,159'	286	260-200, 200-100, 100-50, 50-20, 20-0m

HE605_20-3	BAR-3	21.8	WP3	71° 41,626'	026° 12,197'	326	Wire length 310m
HE605_20-4	BAR-3	21.8	Multi-net	71° 41,462'	026° 14,318'	327	310-200, 200-100, 100-70, 70-50, 50-0m
HE605_20-5	BAR-3	21.8	Bongo	71° 41,184'	026° 18,314'	335	Wire length 502m
HE605_21-8	POR-1	22.8	WP3	70° 31,707'	025° 39,070'	148	Wire length 135m
HE605_21-9	POR-1	22.8	WP3	70° 31,750'	025° 39,454'	147	Wire length 125m
HE605_21-10	POR-1	22.8	Multi-net	70° 31,966'	025° 39,657'	158	142-100, 100-70, 70-50, 50-20, 20-0m
HE605_21-11	POR-1	22.8	Bongo	70° 31,954'	025° 39,162'	168	Wire length 268m
HE605_23-7	POR-3	24.8	WP3	70° 05,279'	025° 06,628'	77	Wire length 60m
HE605_23-8	POR-3	24.8	Multi-net	70° 05,158'	025° 06,263'	67	50-20, 20-10, 10-0m
HE605_23-9	POR-3	24.8	Bongo	70° 05,457'	025° 07,098'	89	75m depth on pressure sensor
HE605_23-10	POR-3	24.8	WP3	70° 05,442'	025° 07,316'	84	72m depth on pressure sensor
HE605_23-11	POR-3	24.8	WP3	70° 05,486'	025° 07,332'	87	76m depth on pressure sensor
HE605_24-9	POR-4	25.8	WP3	70° 18,570'	025° 18,041'	87	77m depth on pressure sensor
HE605_24-10	POR-4	25.8	Multi-net	70° 18,693'	025° 18,109'	81	55-20, 20-10, 10-0m
HE605_24-11	POR-4	25.8	Bongo	70° 18,976'	025° 18,581'	96	85m depth on pressure sensor
HE605_24-12	POR-4	25.8	WP3	70° 19,061'	025° 18,719'	97	86m depth on pressure sensor
HE605_26-8	POR-6	26.8	WP3	70° 53,116'	026° 03,812'	194	Wire length 178m
HE605_26-9	POR-6	26.8	WP3	70° 52,985'	026° 03,761'	194	Wire length 179m
HE605_26-10	POR-6	26.8	Multi-net	70° 53,186'	026° 03,807'	194	183-100, 100-70, 70-50, 50-20, 20-0m
HE605_26-11	POR-6	26.8	Bongo	70° 53,882'	026° 04,217'	194	180m depth on pressure sensor
HE605_27-3	POR-7	26.8	WP3	71° 05,464'	026° 19,743'	164	Wire length 152m
HE605_27-4	POR-7	26.8	Multi-net	71° 05,732'	026° 19,838'	96	90-70, 70-50- 50-20, 20-0m
HE605_27-5	POR-7	26.8	WP3	71° 05,467'	026° 19,731'	163	Wire length 147m
HE605_27-6	POR-7	26.8	Bongo	71° 06,245'	026° 19,716'	148	Wire length 214m
HE605_27-7	POR-7	26.8	Bongo	71° 06,798'	026° 19,495'	199	95m depth on pressure sensor
HE605_29-5	BLC-1	29.8	WP3	69° 30,352'	015° 45,455'	668	Wire length 600m
HE605_29-6	BLC-1	29.8	Multi-net	69° 30,133'	015° 45,663'	601	
HE605_29-7	BLC-1	29.8	Bongo	69° 30,675'	015° 46,860'	532	Wire length 407m
HE605_30-4	BLC-2	29.8	WP3	69° 28,016'	015° 39,068'	1281	Wire length 973m
HE605_30-5	BLC-2	29.8	Multi-net	69° 27,935'	015° 39,266'	1222	Wire length 549m
HE605_31-3	BLC-3	30.8	WP3	69° 29,744'	015° 47,483'	323	Wire length 311m
HE605_31-4	BLC-3	30.8	WP3	69° 29,726'	015° 47,528'	316	Wire length 300m
HE605_31-5	BLC-3	30.8	WP3	69° 29,713'	015° 47,487'	321	Wire length 309m
HE605_31-6	BLC-3	30.8	Multi-Net	69° 29,654'	015° 47,345'	337	Wire length 446m
HE605_31-7	BLC-3	30.8	Bongo	69° 29,025'	015° 44,762'	690	Wire length 468m

On board, all net catches were sorted into different taxonomic groups. Gelatinous taxa were identified, where possible, up to species level, individually photographed, and frozen at -80°C or preserved in 96% undenatured ethanol. Abundances will be calculated based on the volume of water sampled and the number of jellies counted per species.

Other macrozooplankton species, including amphipods, pteropods and decapods were also sorted, counted and subsequently preserved in ethanol. Various taxa were sorted out for experimental work (*Themisto abyssorum*), for contaminant analyses (*Aglantha digitale*, *T. abyssorum*), for molecular diet analyses (*A. digitale*) and for parasite studies (gelatinous zooplankton, chaetognaths). Samples were either preserved in ethanol or frozen at -80°C.

5.3 Sediment sampling for environmental DNA

(I. Rathnayake[1], C. Havermans[1])

[1]AWI

At each station, at least one Van Veen grab deployment was carried out, resulting in a total of 49 grab deployments during the expedition (Table 3). The sediment surface layer was sampled with a sterile spoon, collecting surface sediment in triplicates and collected in sterile falcon tubes, for environmental DNA analyses. At station 4, several grab deployments were done one after the other as not enough sediment was recovered in each of them to obtain the triplicate samples for eDNA. In order to assess small-scale variation in metazoan communities revealed with eDNA metabarcoding, we carried out a sequence of Van Veen Grab deployments at the same position at several stations: 3 grabs at station 10 in Van Mijenfjorden (VMF-1), 3 grabs at station 13 in Hornsund (HORN-1), and 5 subsequent grab deployments at stations 23, 24 and 26 in Porsangerfjorden (POR-3, POR-4 and POR-6, respectively).

Benthic animals were sorted (and photographed) from the sediment samples in Kongsfjorden and Porsangerfjorden. They will be genetically "barcoded" in the home laboratories, in order to construct a reference library of sequences for the eDNA analyses (see Fig. 12.1.1 in Appendix).

Table 3 Details on the Van Veen Grab deployments (coordinates, bottom depth, sampling depths) at each of the stations. The following abbreviations are used for the station localities: KROSS = Krossfjorden, KONG = Kongsfjorden, BIL = Billefjorden, VMF = Van Mijenfjorden, HORN = Hornsund, BAR = Barents Sea, POR = Porsangerfjorden, BLC = Bleik Canyon (Vesterålen).

Station No.		Date	Gear	Latitude	Longitude	Water Depth	Remarks/Recovery
HEINCKE	AWI	2022		[°N]	[°E]	[m]	
HE605_1-2	KROSS-1	15.8	GRAB	79° 11,769'	011° 47,868'	362	Wire length 348m
HE605_2-2	KROSS-2	15.8.	GRAB	79° 07,785	011° 40,606'	330	Wire length NA
HE605_3-2	KONG-1	15.8	GRAB	78° 58,410'	011° 46,439'	216	Wire length NA
HE605_4-1	KONG-2	16.8	GRAB	78° 55,585'	011° 59,631'	91	Wire length 90m
HE605_4-1	KONG-2	16.8	GRAB	78° 55,579'	011° 59,671'	89	Wire length 89m
HE605_4-1	KONG-2	16.8	GRAB	78° 55,573'	011° 59,700'	89	Wire length 86m
HE605_4-1	KONG-2	16.8	GRAB	78° 55,575'	011° 59,710'	91	Wire length 90m
HE605_5-2	KONG-3	16.8	GRAB	78° 56,773'	011° 54,969'	275	Wire length 272m
HE605_7-2	BIL-1	17.8	GRAB	78° 39,758'	016° 43,930'	192	Wire length 180m
HE605_8-2	BIL-2	17.8	GRAB	78° 39,550'	016° 40,632'	190	Wire length 170m
HE605_9-2	BIL-3	17.8	GRAB	78° 37,571'	016° 33,334'	138	Wire length 130m
HE605_10-2	VMF-1	18.8	GRAB	77° 45,764'	015° 08,389'	105	Wire length 101m
HE605_10-3	VMF-1	18.8	GRAB	77° 45,776'	015° 08,292'	104	Wire length 99m
HE605_10-4	VMF-1	18.8	GRAB	77° 45,768'	015° 08,267'	104	Wire length 100m
HE605_11-2	VMF-2	18.8	GRAB	77° 47,950'	015° 20,284'	105	Wire length 102m
HE605_12-2	VMF-3	18.8	GRAB	77° 46,145'	015° 16,904'	100	Wire length 96m
HE605_13-2	HORN-1	19.8	GRAB	76° 59,797'	016° 26,880'	126	Wire length NA
HE605_13-3	HORN-1	19.8	GRAB	76° 59,828'	016° 26,786'	125	Wire length NA
HE605_13-4	HORN-1	19.8	GRAB	76° 59,825'	016° 26,776'	125	Wire length NA
HE605_14-2	HORN-2	19.8	GRAB	76° 59,499'	016° 00,600'	106	Wire length 104m
HE605_15-2	HORN-3	19.8	GRAB	76° 57,757'	015° 49,603'	222	Wire length 203m
HE605_18-2	BAR-1	21.8	GRAB	72° 16,749'	024° 26,258'	267	Wire length 257m
HE605_19-3	BAR-2	21.8	GRAB	71° 48,761'	025° 34,394'	280	Wire length NA
HE605_20-2	BAR-3	21.8	GRAB	71° 41,635'	026° 12,171'	325	Wire length NA
HE605_21-7	POR-1	22.8	GRAB	70° 31,680'	025° 39,192'	146	Wire length 136m
HE605_23-2	POR-3	24.8	GRAB	70° 05,270'	025° 06,650'	77	Wire length 78m
HE605_23-3	POR-3	24.8	GRAB	70° 05,260'	025° 06,615'	75	Wire length 78m
HE605_23-4	POR-3	24.8	GRAB	70° 05,258'	025° 06,560'	75	Wire length 77m
HE605_23-5	POR-3	24.8	GRAB	70° 05,266'	025° 06,526'	75	Wire length 76m
HE605_23-6	POR-3	24.8	GRAB	70° 05,275'	025° 06,522'	75	Wire length 75m
HE605_24-2	POR-4	25.8	GRAB	70° 18,593'	025° 18,031'	85	Wire length 84m

HE605_24-3	POR-4	25.8	GRAB	70° 18,586'	025° 18,025'	87	Wire length 85m, no sample
HE605_24-4	POR-4	25.8	GRAB	70° 18,598'	025° 17,999'	84	Wire length 84m, no sample
HE605_24-5	POR-4	25.8	GRAB	70° 18,565'	025° 18,006'	88	Wire length 89m
HE605_24-6	POR-4	25.8	GRAB	70° 18,521'	025° 18,022'	89	Wire length 89m
HE605_24-7	POR-4	25.8	GRAB	70° 18,503'	025° 18,084'	88	Wire length 89m
HE605_24-8	POR-4	25.8	GRAB	70° 18,528'	025° 18,072'	88	Wire length 88m
HE605_26-2	POR-6	26.8	GRAB	70° 53,246'	026° 04,099'	193	Wire length 187m
HE605_26-3	POR-6	26.8	GRAB	70° 53,235'	026° 04,016'	193	Wire length 188m
HE605_26-4	POR-6	26.8	GRAB	70° 53,226'	026° 03,972'	193	Wire length 187m
HE605_26-5	POR-6	26.8	GRAB	70° 53,222'	026° 03,941'	193	Wire length 188m
HE605_26-6	POR-6	26.8	GRAB	70° 53,202'	026° 03,888'	193	Wire length 190m
HE605_26-7	POR-6	26.8	GRAB	70° 53,184'	026° 03,844'	194	Wire length 188m
HE605_27-2	POR-7	26.8	GRAB	71° 05,448'	026° 19,775'	174	Wire length 178m
HE605_27-2	POR-7	26.8	GRAB	71° 05,450'	026° 19,766'	171	Wire length 178m
HE605_27-2	POR-7	26.8	GRAB	71° 05,451'	026° 19,756'	172	Wire length 174m, no sample
HE605_29-3	BLC-1	29.8	GRAB	69° 30,351'	015° 45,482'	660	Wire length 688m, no sample
HE605_29-4	BLC-1	29.8	GRAB	69° 30,356'	015° 45,468'	664	Wire length 675m, no sample
HE605_30-3	BLC-2	29.08	GRAB	69° 28,054'	015° 39,007	1290	Wire lemgth 1293m

5.4 Trophic ecology of jellyfish and fish

(I. Stoltenberg[1], A. Dischereit[2])

[1]GEOMAR

[2]AWI

Different aspects of the Arctic marine food web, with a key focus on GZP, were investigated in the course of the HE605 expedition. We aimed to investigate the role of GZP as 1) prey for different fish species in open water and fjord systems, and 2) as predators of other zooplankton. This will be done using biomarker studies and molecular diet analyses (DNA metabarcoding). Besides investigating the trophic role of GZP in the different ecosystems visited, we also aim to evaluate their nutritious value.

For the biomarker analyses, we sampled different food web components: seston, using the CTD/rosette water sampler, three different zooplankton size classes (300-500 µm, Multi-net; 500-1000 µm, Bongonet; >1000 µm, WP3 net, Fig. 5.1), and large scyphozoan jellyfish (e.g. *Cyanea*, *Aurelia*) and fish (hand nets, scientific angling, respectively) at three different stations (3, 13, 20) in Kongfjorden, Hornsund and the Barents Sea.

We collected fish for molecular diet and biomarker analyses using scientific angling at different localities from the outer shelf of Kongsfjorden to northern Norway (Fig. 5.2a). Scientific angling is the most appropriate method for diet studies, as it overcomes the typical bias associated to net feeding. Stomachs were removed from the fish and frozen at -80°C. Length was measured and sex was determined for each fish caught. In total, we collected 62 specimens belonging to different species: 56 individuals of Atlantic cod (*Gadus morhua*), 2 individuals of halibut (*Hippoglossus hipoglossus*), 2 individuals of redfish (*Sebastes* sp.), 1 individual of haddock (*Melanogrammus aeglefinus*), and 1 individual of pollock (*Pollachius pollachius*). A muscle tissue sample was also collected for each fish and frozen at -80°C. This will be used for complementary biomarker analyses (biomarkers, stable isotopes) to determine the trophic signal of the fish, integrated over a longer time frame than the molecular diet studies (representing a temporal snapshot). Finally, we also aim to investigate the diet of a dominant hydrozoan species, *Aglantha digitale* with DNA metabarcoding. These samples were collected with different types of plankton nets at six different locations (Fig. 5.2b). At each location, ca. 20 specimens were length-measured. Of each specimen, the manubrium was dissected and isolated. In order to avoid cross-contamination between individuals and locations, dissection instruments were cleaned using DNA Exitus and ethanol. The isolated stomachs and the remaining bell were frozen separately at -80°C for further examination in the home laboratories.

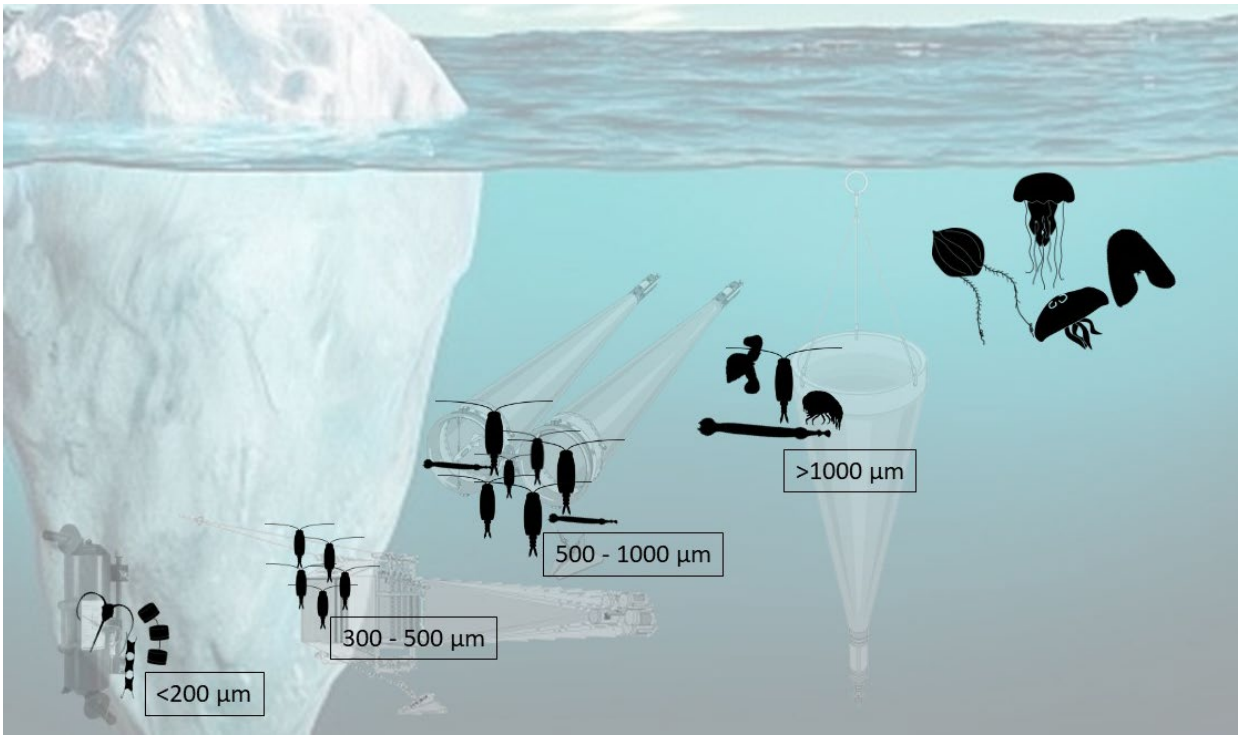

Fig. 5.1 Different size fractions sampled for biomarker analyses with different gear: seston was collected with the CTD/Rosette water sampler, zooplankton with the Multi-net, Bongo net and WP3, and larger jellyfish and fish with hand nets and scientific angling (I. Stoltenberg).

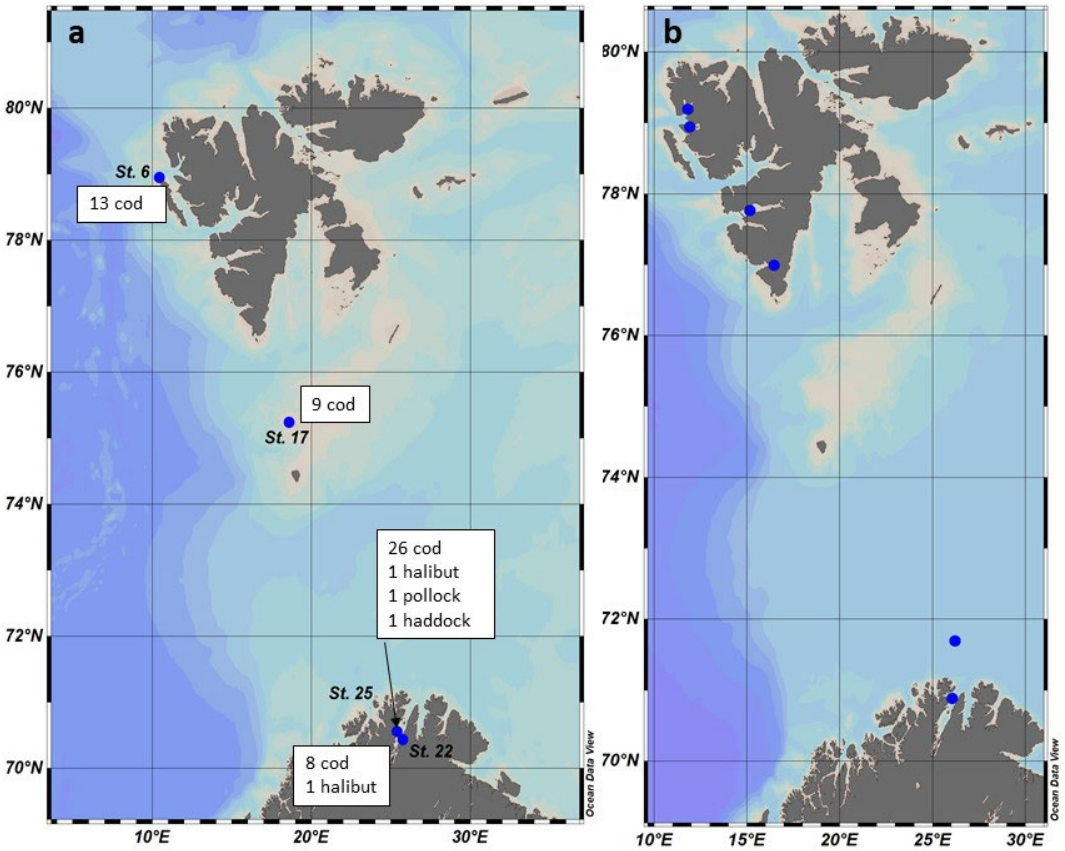

Fig. 5.2 **a.** Sampling localities where different fish species were caught using scientific angling, and **b.** Sampling sites for *Aglantha digitale* specimens collected for DNA metabarcoding analyses.

5.5 Camera deployments for in-situ observations

(C. Havermans[1], A. Dischereit[1], H.J. Hoving[2], H. Hampe[2])

[1]AWI

[2]GEOMAR

Over recent years, methodological developments have optimized the use of optical platforms for assessing GZP, allowing to obtain more reliable abundance estimates (Hoving et al. 2019), to assess fine-scale horizontal and vertical distributions and to provide biological information on behavior (Hoving et al. 2013) and on species interactions (e.g., Hoving & Haddock 2017).
During the HE605 cruise, we deployed the towed camera system Pelagic In Situ Observation System PELAGIOS II (Hoving et al. 2019) to perform pelagic video transects down to 300 m water depth. This system was towed horizontally via the fibre optic cable at low ships speed (1 knot) at different depths from 300 m to just beneath the surface. The PELAGIOS II consists of both a 4k and HD camera, a depth sensor with current meters, and a CTD. The water column in front of the camera is illuminated by LED lights. It was deployed at 6 stations, including one survey each in Krossfjorden, Kongsfjorden, Hornsund, Barents Sea, and at two localities in Porsangerfjorden (see Table 4).
We also deployed the Ocean Floor Observation System OFOS in order to characterize the benthic fauna, as well as the presence of jellyfish carcasses (so called "jelly-falls) on the seafloor. Because of a combination of high biomass and an assumingly low predation pressure following a bloom event, sinking GZP carcasses can be important vectors of carbon to the seafloor (Lebrato et al. 2013). This has been documented for fjord and continental shelf systems (Yamamoto et al. 2008; Sweetman & Chapman 2011). Once on the seafloor, these jelly-falls may sustain a diverse benthic scavenging community, such as crustaceans (Dunlop et al. 2017; Havermans and Smetacek 2018).
Finally, the BlueROV2 remotely operated vehicle was deployed in Porsangerfjorden at one single location. Weather and swell conditions and other operations prevented further deployments of the zodiac for ROV surveys during the cruise. Vertical dives were carried out during which large scyphozoan jellyfish such as *Cyanea* sp. were observed.
All video data will be annotated using the video and annotation reference system VARS.

Table 4 Details on the deployments of the different optical platforms: PELAGIOS, OFOS and the BlueROV2, with the coordinates, bottom depth, sampling depths and profiles achieved at each of the stations. The following abbreviations are used for the station localities: KROSS = Krossfjorden, KONG = Kongsfjorden, BIL = Billefjorden, VMF = Van Mijenfjorden, HORN = Hornsund, BAR = Barents Sea, POR = Porsangerfjorden.

Station No.		Date	Gear	Latitude	Longitude	Water Depth	Remarks
HEINCKE	AWI	2022		[°N]	[°E]	[m]	
HE605_1-5	KROSS-1	15.8	PELAGIOS	79° 12,230'	011° 48,984'	309	Profiles at 300, 200, 100, 70, 50, 20m
HE605_5-5	KONG-3	16.8	PELAGIOS	78° 56,775'	011° 54,472'	233	Profiles at 200, 100, 70, 50m
HE605_9-5	BIL-3	17.8	OFOS	78° 37,442'	016° 32,716'	147	1h:00min profile above seafloor
HE605_12-5	VMF-3	18.8	OFOS	77° 48,376'	015° 19,359'	103	1h:17min profile above seafloor
HE605_13-8	HORN-1	19.8	OFOS	76° 59,838'	016° 27,057'	125	0h:58min profile above seafloor
HE605_16-1	HORN-4	19.8	PELAGIOS	76° 59,266'	015° 49,480'	200	Profiles at 180, 100, 70, 50, 20m
HE605_18-5	BAR-1	21.8	PELAGIOS	72° 17,892'	024° 27,466'	268	Profiles at 200, 100, 70, 50, 20m
HE605_21-12	POR-1	22.8	BlueROV2	70° 31,865'	025° 39,052'	158	Vertical survey at 0-30m
HE605_23-12	POR-3	24.8	OFOS	70° 05,294'	025° 06,545'	77	1h:00min profile above seafloor
HE605_23-13	POR-3	24.8	PELAGIOS	70° 06,501'	025° 09,047'	104	Profiles at 90, 70, 50, 20, 5, 3m
HE605_24-13	POR-4	25.8	OFOS	70° 19,126'	025° 18,271'	96	0h:57min profile above seafloor
HE605_24-14	POR-4	25.8	PELAGIOS	70° 19,865'	025° 19,635'	84	Profiles at 85, 100, 70, 50, 20, 10, 5, 1m
HE605_26-12	POR-6	26.8	OFOS	70° 54,364'	026° 04,366'	194	0h:46min profile above seafloor

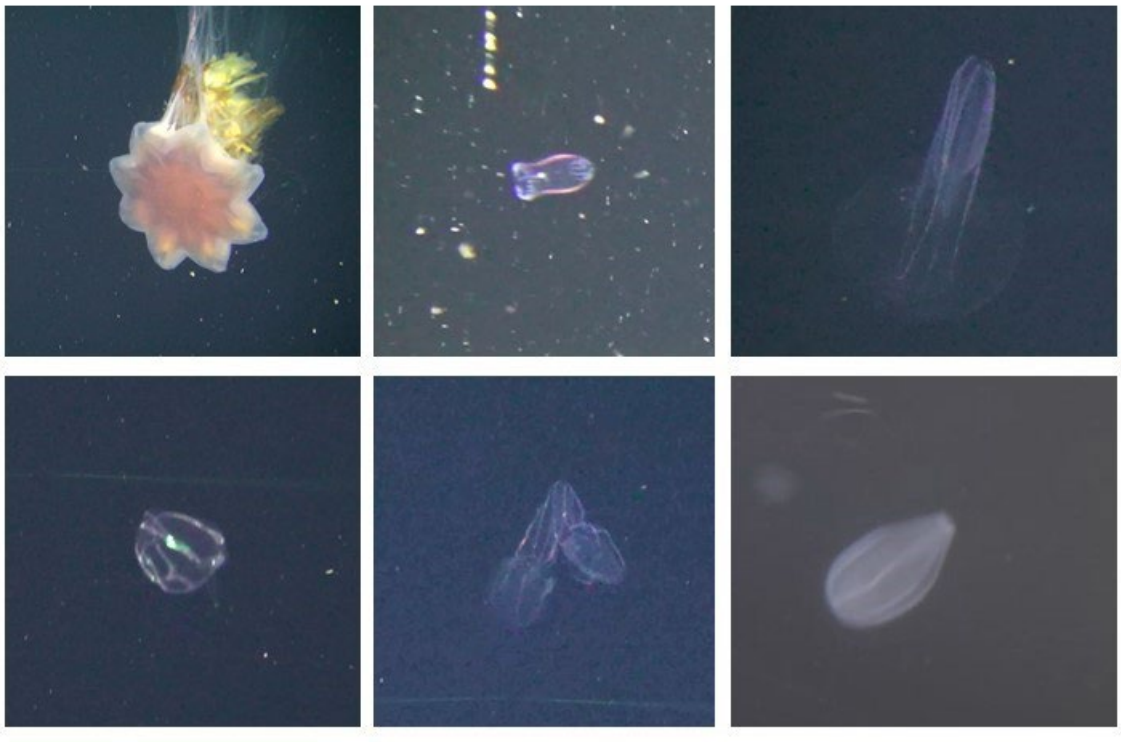

Fig. 5.3 Different gelatinous zooplankton species observed in the water column and above the seafloor with the towed pelagic camera PELAGIOS and the seafloor camera system OFOS.

Fig. 5.4 Decapod taxa observed with the Ocean Floor Observation System OFOS: the Norwegian red king crab (*Paralithodes camtschaticus*) and unidentified shrimps.

5.6 Microplastic analyses on zooplankton along a poleward gradient

(C. Havermans[1], A. Dischereit[1])

[1]AWI

Microplastics are abundant and widespread in the marine environment, as a result from various processes, including the degradation of larger pieces of plastic (Thompson et al. 2004). Due to their small size, microplastics are potentially bioavailable and can be ingested by a wide range of organisms, when they overlap with the size of their prey (Galloway et al. 2017; Botterell et al. 2019). Coastal areas and shelf regions have been identified as hotspots of microplastic accumulation, and zooplankton, occurring in high abundances, will be at increased risk of microplastic ingestion (Botterell et al. 2019). As zooplankton are a crucial food source for many

secondary consumers, they represent a route of microplastic transfer to higher trophic levels, including commercially exploited fish species (Botterell et al. 2019).

During HE605, we sampled two very abundant zooplankton taxa that were found at different localities along the latitudinal gradient from high-Arctic to Atlantic waters. These taxa were the hyperiid amphipod *Themisto abyssorum*, and the hydrozoan *Aglantha digitale*. Twenty individuals of each taxon were caught with different plankton nets (WP3 and Bongo nets) at each of the following sites: Kongsfjorden, (st. 5), Hornsund (st. 13 and 14), Bleik Canyon (st. 30). With this sample set, we will be able to assess and compare the incidence of ingestion of microplastics (number of organisms that ingested microplastics/total number of organisms processed; Steer et al. 2017) between species and between localities and water regimes. Microplastic polymers inside the zooplankton specimens will be detected and identified using Micro Fourier Transformed Infrared Spectroscopy (µ-FTIR). Zooplankton samples will be carefully cleaned before digestion. Part of these specimens may also be used for other contaminant studies.

When handling the sampled specimens, we wore nitrile (plastic-free) gloves and cotton labcoats. In order to evaluation the sources of external, ship-board contamination, we used wetted 0.2 µm polycarbonate filters (for airborne filters) exposed in glass petri slides which were placed 1) at the corner of the working bench where samples were handled and 2) and the entrance of the door of the room where specimen sorting took place. It was opened from the beginning of the sorting and closed at the end when storing the zooplankton samples; the time of the opening until closing of the petri slide was recorded. Zooplankton specimens were stored separately into empty plastic bags (whirl-pack) and stored at -80°C. Contaminant sources were identified, photographed, and individual scrapings were taken ("contamination library"), e.g., from the plastic sample storage bags, as well as scrapings from the deck polymeric paintings, plastic from the plankton net components and from working clothes used during sampling. These potential contaminant-polymers were scraped with metal pincers, and stored into glass vials that were frozen at 80°C, similar to the zooplankton samples. The same was done with empty plastic sample bags.

5.7 Stressor experiments with the amphipod *Themisto abyssorum*

(V. Stenvers[1], H. Hauss[1], H.-J. Hoving[1])

[1]GEOMAR

[2]National Museum of Natural History, Smithsonian Institution, Washington DC, USA

The commercial interest to mine minerals on the deep-seabed has increased substantially in the past years. Although the plans to commercially mine minerals from the deep-seabed are well underway, many questions remain about the environmental impact to deep-sea ecosystems (Washburn et al. 2019; Christiansen et al. 2020; Drazen et al. 2020). In particular, sediment plumes generated during deep-sea mining are suggested to have devastating effects on animals living in the water column (Drazen et al. 2020).

To assess the effects of sediment plumes on midwater animals, pilot experiments were conducted with the hyperiid amphipod *Themisto abyssorum* (Boeck, 1871) (Fig. 5.5a). These experiments are part of a larger study to investigate the effects of deep-sea mining on midwater animals within the iAtlantic consortium, including fellows from the GEOMAR Helmholtz Centre for Ocean Research Kiel and Heriot-Watt University (Stenvers & Hauss et al. unpublished results). Individuals of *Themisto abyssorum* (149 in total) were collected in all fjords surrounding Svalbard and exposed to five different sediment treatments (0, 16.7, 33.3, 166.7, 333.3 $mg \cdot L^{-1}$). Incubations lasted 24 hours using previously collected abyssal plain sediment from the North

East Atlantic at 4500 m depth. The consumption of oxygen was measured every six hours in respiration bottles attached to a rotating plankton wheel (Fig. 5.5b), containing one to five *T. abyssorum* depending on bottle size (either 50ml or 100ml). All experiments were done at 4°C while bottles were wrapped in aluminum foil to keep the animals dark adapted. Our first results indicate that different sediment concentrations have a marked effect on oxygen consumption. Further work, including the determination of dry mass and morphometric dimensions of individual specimens, will be conducted at GEOMAR. These experiments are few of the first to investigate the respiratory response of midwater crustaceans to deep-sea mining induced sediment plumes (van der Grient & Drazen 2022).

This project has received funding from the European Union's Horizon 2020 research and innovation programme under grant agreement No 818123 (iAtlantic).

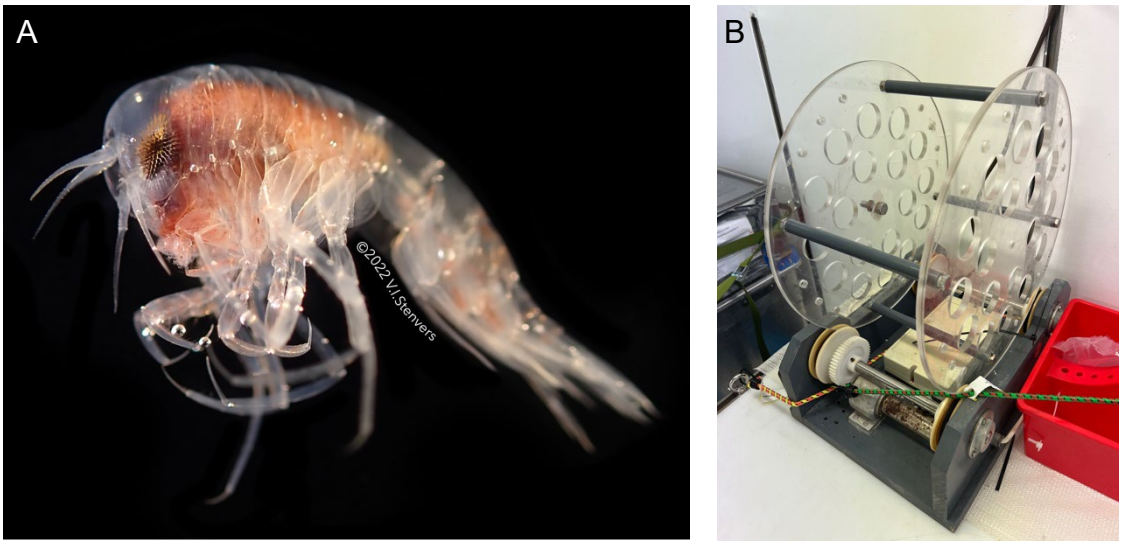

Fig. 5.5 **a.** The hyperiid amphipod *Themisto abyssorum*, and **b.** the plankton wheel used for the experiments.

5.8 Expected results

5.8.1 Metazoan communities across a latitudinal gradient with eDNA analyses

(C. Havermans[1], A. Eschbach[1], A. Murray[1], R. Gorniak[1], H.J. Hoving[2])

[1]AWI

A total of 31 CTD casts were carried out, resulting in 518 Sterivex filters for eDNA analyses. From the 49 Van Veen Grab deployments, 114 sediment samples were obtained for eDNA analyses. In the AWI home laboratories, DNA will be extracted from these filters and from the sediment samples. PCR amplification will be performed with triplicates on these samples. We will apply universal primers, including primers targeting the v1-2 region of 18S rRNA (Günther et al., 2021) and primers targeting a 313-bp fragment (the commonly used "Leray fragment") of the cytochrome *c* oxidase subunit I (COI) gene (Leray et al. 2013). The variable 18S rRNA v1-2 region is known to target gelatinous zooplankton groups well (Günther et al., 2021) whereas the barcode region of mitochondrial COI will provide a finer assay of metazoan community diversity in general (Questel et al., 2021). Whereas the 18S rRNA fragment appears to be more efficient in detecting tunicates and ctenophores, the Leray COI primers have been proven useful for discriminating a wide range of cnidarian species (Rathnayake, 2022). After the PCR amplification, libraries will be prepared for sequencing on a MiSeq/NovaSeq Illumina sequencing platform. The DNA reads generated will be processed and clustered into operational

taxonomic units using bioinformatic pipelines. Statistical analyses will be applied to evaluate the differences in taxonomic composition as well as regional differences in metazoan communities and species richness. In the GEOMAR laboratories, the DNA extracts will be used for applying DNA metabarcoding with primer sets targeting cephalopod species (de Jonge et al. 2021).

5.8.2 Short-term temporal variation of metazoan environmental DNA

(C. Havermans[1], R. Gorniak[1], Ayla Murray[1], Andrea Eschbach[1])

[1]AWI

Environmental DNA sampling has become as a powerful tool to detect and monitor biodiversity in marine ecosystems in a non-invasive way, providing detailed, accurate and fine-scale information on marine pelagic and benthic communities. Different applications of eDNA tools have been developed for marine metazoan studies, such as, for example, detection of elusive, endangered, rare or invasive species, providing estimates of species richness, monitoring of community changes (Havermans et al. 2022). Biodiversity surveys of pelagic communities is often achieved using a CTD/rosette sampler for water sampling, followed by DNA extraction and metabarcoding of the filtered seawater. Nevertheless, studies addressing the reliability of eDNA water sampling methods and the temporal variation of eDNA in the water column are rare (e.g., Jensen et al. 2022). Consequently, we aim to determine a) if and how the metazoan community composition across the water column varies in a time span of a couple of hours as well as between specific depths, and b) if one CTD/rosette sampler deployment can comprehensively identify the local metazoan diversity in a dynamic fjord system (Fig. 5.6). For this purpose, six rosette water sampler deployments were carried out successively, sampling at five different depths across the water column, at the same location in Porsangerfjorden (station 21, POR-1). For each depth, 3x 2L was filtered over a Sterivex filter, resulting in triplicate samples per depth per deployment. The metazoan species richness will be determined using the mitochondrial cytochrome *c* oxidase I (COI) gene (same primer set as for section 5.8.1). Technical PCR triplicates will be prepared during the library preparation; the Illumina MiSeq platform will be used for sequencing. This dataset will allow a comparison of the metazoan communities and dominant species observed between the different time frames (the ca. 2h30 time period between deployment 1 and 6) and between the different depths sampled (surface layer, 20m, 50m, 70m, 100m, 135m water depths).
A similar comparison of metazoan diversity will be carried out on the sediment samples, for the stations at which 3-5 subsequent Van Veen grabs were deployed at the same position (VMF-1, HORN-1, POR-3, POR-4, POR-6). This will help to better estimate the impact of local spatial variability in eDNA for revealing sediment communities.

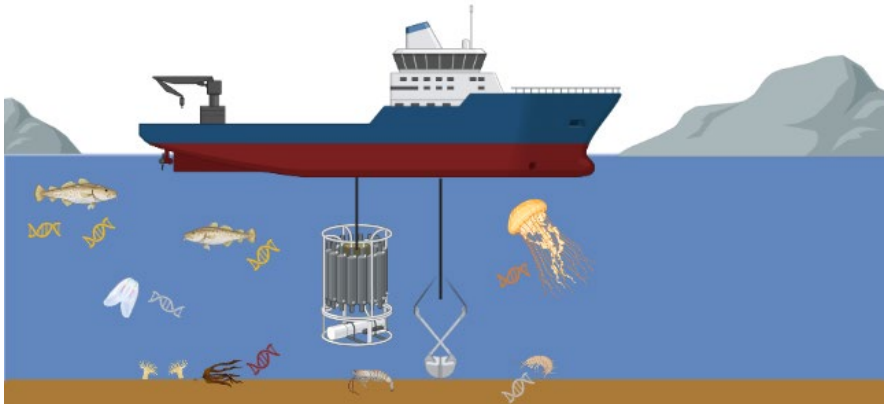

Fig. 5.6 A graphical representation of eDNA sampling carried out during HE605.

5.8.3 Abundance and diversity of gelatinous zooplankton

(A. Hosia[1], J.J. Soto-Angel[1], C. Havermans[2])

[1]UiB

[2]AWI

For vertically stratified abundances of GZP, Multinet samples from stations indicated in Fig. 5.7 were processed quantitatively right after sampling. Live samples were observed over a light table, and all gelatinous organisms were picked, quantified, and identified to lowest possible taxon with the help of a stereomicroscope. Additional data on species diversity was recovered from the WP3 net samples. Deploying the WP3 net vertically with a low towing speed (0.2 ms^{-1}) is a relatively gentle method of net sampling, and the WP3 was able to retrieve a larger number of gelatinous species compared to the Multinet or the Bongo net. The WP3 samples were processed qualitatively for species composition, with the live samples observed over a light table. A few additional species were also found during a cursory visual control of the Bongo net samples, and *Staurostoma mertensii* was observed and collected using dip-nets in mid-Porsangerfjorden, between stations 23 and 24.

A selection of >250 net-caught specimens representing most cnidarian and ctenophore species observed during the expedition were individually documented for morphology alive with a camera attached to a stereomicroscope and/or macrophoto prior to fixation in 99% ethanol for later molecular work. The samples will be used for DNA barcoding of COI and 16S sequences with photographic vouchers, to be made openly accessible in reference sequence databases for Arctic gelatinous zooplankton. Collected morphological and molecular data will further be used to resolve existing taxonomic questions, and a few samples for selected taxa were also fixated in 4% borax buffered formalin in sea water for later morphological work.

A total of >35 taxa of ctenophores and cnidarians were observed during the cruise (Fig. 5.8 and 5.9). The *Beroe* spp. ctenophores include both morphotypes *B.* cf. *cucumis* and *B.* cf. *abyssicola*, the taxonomy of which is currently uncertain. A ctenophore specimen belonging to a genus pending description (Majaneva, Hosia et al., unpublished results) was also collected at van Mijenfjorden. Highest densities were found at station 27 in Porsangerfjorden (Fig. 5.7), where there were abundanct physonect siphonophores and numerous *Clytia* sp., as well as at Hornsund, with abundant *Aglantha digitale*.

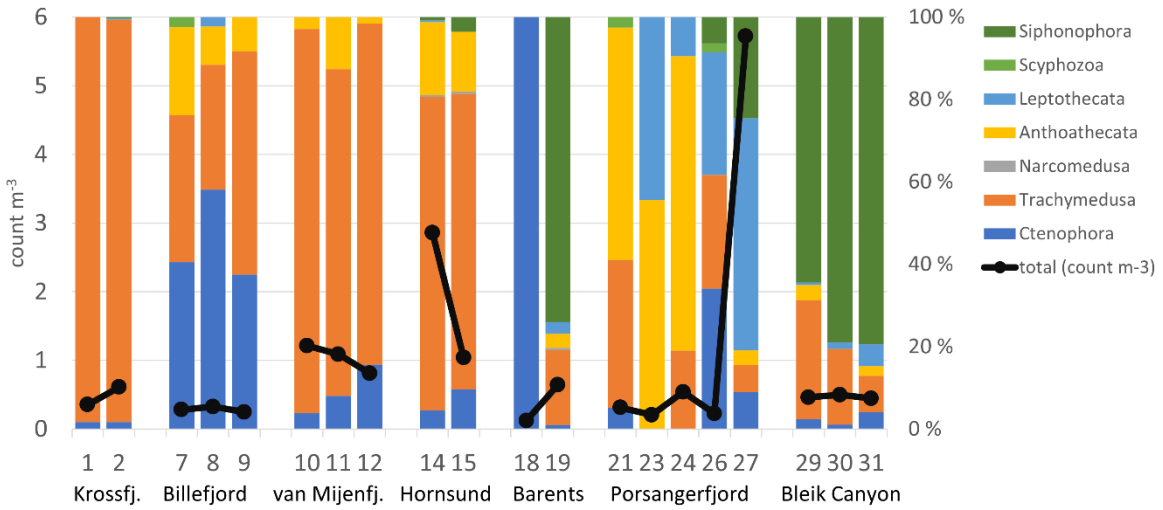

Fig. 5.7 Average combined density (count.m^{-3}) of ctenophores and cnidarians and percentage contribution of different groups over the entire water column at stations with quantitative multinet sampling. Note that individual nectophores are counted for physonect siphonophores, even though these may come from a single colony.

Aglantha digitale was the only species observed at all stations, while *Beroe* spp. were observed on all stations except for two in Porsangerfjorden. The species count (not normalized for sampling effort) increased towards the southern stations, with the Porsangerfjorden area having the highest total number of species (Fig. 5.8). Pronounced environmental gradients along the fjord likely contributed to this diversity, with the resulting change in community composition from station to station (Fig. 5.7). The outermost station at Porsangerfjorden and the Vesterålen stations were characterized by large numbers of siphonophores, particularly physonects. A large number of detached physonect nectophores in these stations poses a challenge to estimating abundances. Predominantly Arctic species were observed in Billefjorden, van Mijenfjorden, Hornsund, and in the Barents Sea (Fig. 5.8). In addition to several species of hydromedusae with Atlantic affinities, *Tomopteris* polychaetes and collodarian radiolaria were observed in the Barents Sea, Porsangerfjorden and Vesterålen, while doliolids were found in the outer station at Porsangerfjorden and in Vesterålen, indicating a more Atlantic influence in these areas. Further analyses will combine the community composition and abundance data from the net samples with temperature and salinity data from the CTD to look at associations of the gelatinous fauna with Arctic and Atlantic water masses within the study area.

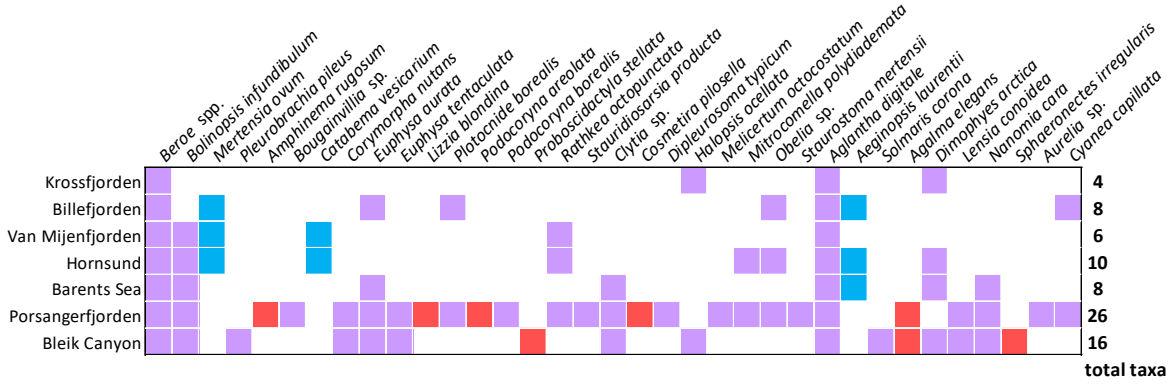

Fig. 5.8 Cnidarians and ctenophores observed at the different sampling areas and the total number of taxa observed in net catches in each area. Data from all nets combined. Blue indicates predominantly Arctic species, red warm water species, and violet species with wide or cosmopolitan distributions including Arctic and other domains (following Ronowicz et al. 2015 and Kramp 1959).

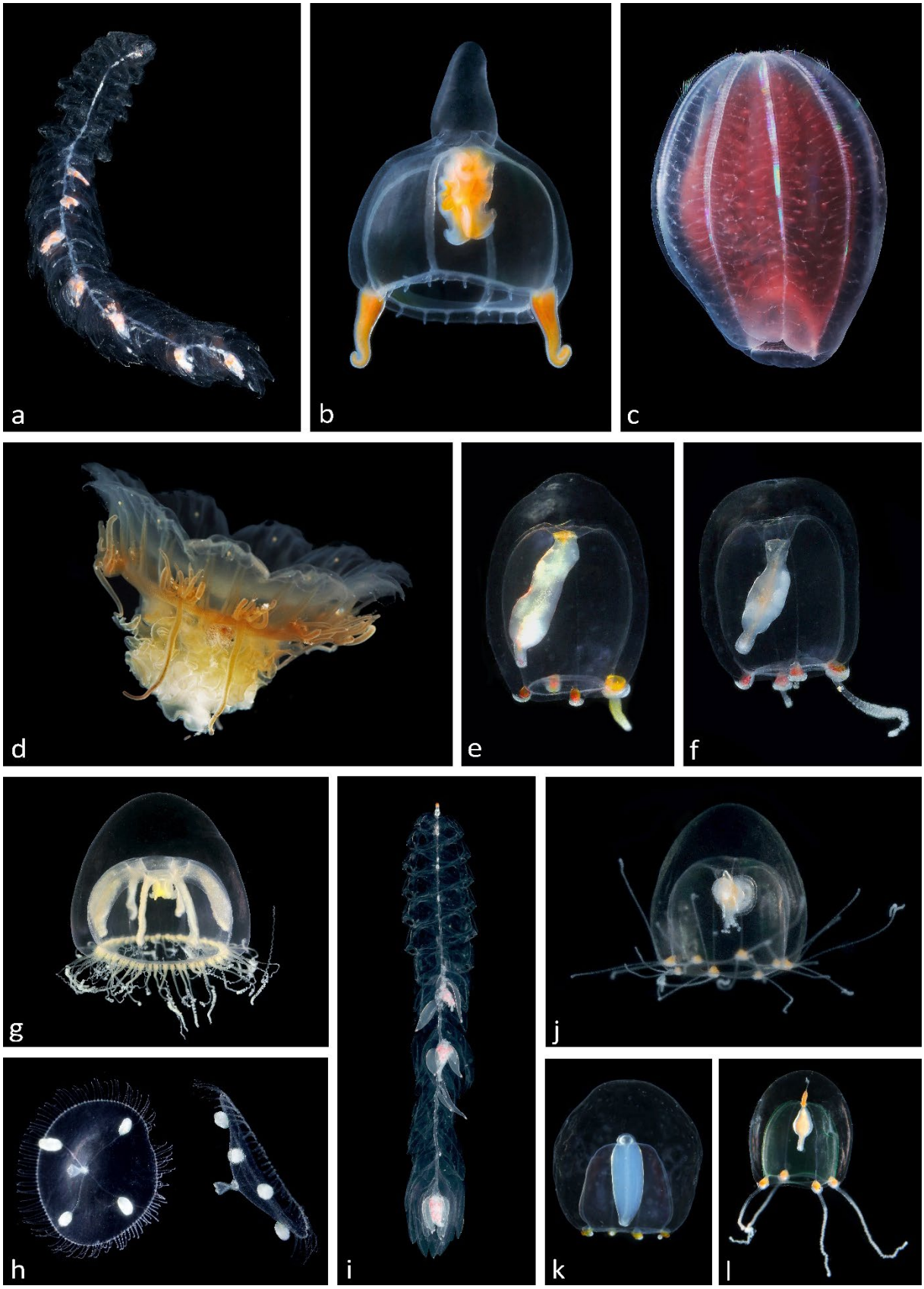

Fig. 5.9 Some of the cnidarian and ctenophore species sampled during HE605. a. *Agalma elegans*, b. *Amphinema rugosum*, c. *Beroe* cf. *abyssicola*, d. *Cyanea capillata*, e. *Euphysa aurata*, f. *Euphysa tentaculata,* g. *Melicertum octocostatum*, h. *Obelia* sp., i. *Nanomia cara*, j. *Rathkea octopuntata*, k. *Plotocnide borealis*, l. *Stauridiosarsia producta.*

5.8.4 Evolutionary origin of bipolarity in Hydrozoa (Cnidaria)

(J.J. Soto-Angel[1], L. Martell[1], C. Havermans[2] A. Hosia[1])

[1]UiB

[2]AWI

Bipolarity is defined as the presence of the same species in both poles, normally absent from lower latitudes (Stepanjants et al. 2006). This phenomenon is a major speciation process over oceanic scale, and the greatest disjunct distribution pattern on earth (Crame 1993). Even though bipolarity was documented nearly two centuries ago, it has been rarely evaluated in an evolutionary context (Allcock & Griffiths 2014). The evolutionary origin and diversification of bipolar taxa is still mostly unknown for most cases. While fossil evidence suggests that bipolarity arose multiple times, the lack of robust phylogenies and estimates of divergence time have often hampered the evaluation of the role of climatic, geological and ecological forces in shaping bipolar distributions, as well as elucidating the time scale in which these speciation events took place (cf. Allcock & Griffiths 2014)

The wide array of life cycle strategies displayed within Hydrozoa (Cnidaria) makes them an ideal group to test several evolutionary and ecological hypotheses under comparative approaches. The Marie Sklodowska-Curie Actions, Individual Fellowship (European Commission, Horizon2020) project POLE2POLE aims to study whether bipolarity-driven speciation is influenced by life cycle strategies using different hydrozoan species as a model.

Dimophyes arctica is a calycophoran siphonophore with a bipolar distribution, very common in both Arctic and Antarctic waters and their subpolar counterparts (Stepanjants et al. 2006). During HE605, a total of 130 specimens of *Dimophyes arctica* (including polygastric and eudoxic stages) have been sampled from different stations within Svalbard and Bleik Canyon (Vesterålen). A selection of 50 specimens was documented alive (Fig. 5.10) for morphological characterization and morphometric analyses and individually preserved for further molecular work. The totality of samples obtained were preserved in 99% ethanol and will be processed for Sanger and High Throughput Sequencing. Subsequent phylogenetic and species delimitation analyses including the North Sea, Antarctic and Sub-antarctic specimens available will reveal how many lineages exist within the current concept of *D. arctica* and its phylogeographic structure.

POLE2POLE project is funded by the Marie Skłodowska-Curie Actions MSCA programme, Horizon2020, European Commission (Grant code: 101031845).

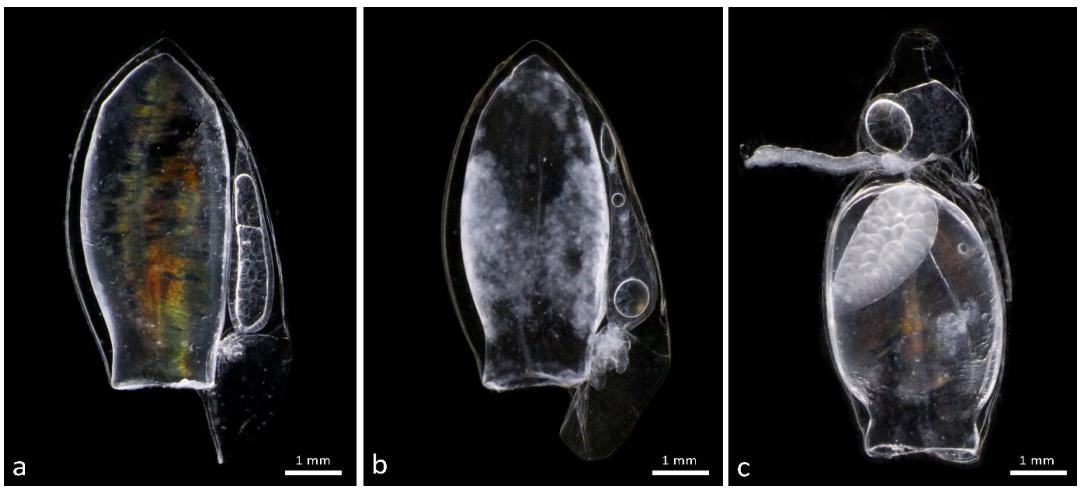

Fig. 5.10 The calycophoran siphonophore *Dimophyes arctica*. **a-b** Anterior nectophore, polygastric stage, **c** eudoxid stage.

5.8.5 Diet analyses of jellyfish and fish using DNA metabarcoding

(A. Dischereit[1], C. Havermans[1])

[1]AWI

In order to evaluate the role of GZP as both prey and predator, we will carry out DNA metabarcoding analyses on stomach contents of both fish and hydrozoan jellyfish, respectively. Stomachs of five species of fish and one dominant and widespread hydrozoan species (*Aglantha digitale*) were isolated on board the expedition (see section 5.4) and preserved at -80°C. To evaluate the prey spectrum these taxa, DNA metabarcoding will be applied, using a universal metazoan primer set, targeting a 313-bp fragment of the mitochondrial COI fragment. The methodology will be similar to the work flow applied for the eDNA analyses (see section 5.8.1) Additionally, the muscle tissues of fish, and the remaining bell of the hydrozoan specimens will be used for biomarker studies. The prey composition dataset of *A. digitale* will be part of a larger study covering Fram Strait (RV Polarstern expedition PS126), and sampling conducted in Kongsfjorden during the Polar Night (AWIPEV KOP183). Hence, we will be able to assess variation in feeding across different regions, water regimes (Atlantic vs. Arctic) and between seasons (summer vs winter).

5.8.6 Trophic ecology of jellyfish using biomarker analyses

(I. Stoltenberg[1])

[1]GEOMAR

For the planned biomarker studies, sampling for the different food web components was carried out at three different sampling sites represent different habitats, including coastal fjord systems that are either influenced by Atlantic water masses (Kongsfjorden) or characterized as an Arctic system (Hornsund) as well as an open ocean system (Barents Sea). The sampling comprised the different size components of the trophic chain: ranging from seston, over three different zooplankton size classes (300-500 µm; 500-1000 µm; >1000 µm) to larger jellyfish and fish.
The resulting sampling set will be analyzed for stable isotopes and fatty acids, two trophic tracers that allow the determination of trophic positions (stable isotopes $\delta^{15}N$) of jellyfish, trace contributions of different prey sources (stable isotopes $\delta^{13}C$; fatty acid values) to the jellyfish diets and the nutritional quality (fatty acids) of jellyfish as a prey item for other planktonic and nektonic predators. Eventually, the results will provide essential baseline data of Arctic jellyfish trophic markers against which future differences in the rapidly changing Arctic Ocean can be measured.

5.8.7 Diversity and prevalence of parasites associated with Chaetognatha

(A. Hosia[1], J.J. Soto-Angel[1], C. Havermans[2], L. Martell[1])

[1]UiB

[2]AWI

Chaetognaths have been considered potential intermediate hosts for several parasites, including different species of helminths and nematodes (Pearre 1979, Øresland 1986, Svendsen 1990, Daponte et al. 2008). However, little is known about their prevalence and specificity, especially for Arctic waters.
Parasites of chaetognaths were sampled for the Norwegian Taxonomy Initiative project "Metazoan parasites of non-crustacean zooplankton" (ParaZoo, PI Luis Martell). The total number of chaetognaths per net (mean 75, range 0-746) was counted from all Multinet samples processed quantitatively for gelatinous zooplankton. A subsample of ~25 chaetognaths from each

Multi-net sample was screened live for parasites (Fig. 5.11) under a stereomicroscope. Individuals with parasites were documented using a camera attached to a stereomicroscope and fixed in 99% ethanol for DNA-based species identification of the host chaetognath and the parasite. In total, 1761 chaetognaths were screened from the Multi-net samples, with ~2.4% found carrying one or more parasites. Additional samples of chaetognaths with parasites were picked from the other nets (WP3, Bongo) non-quantitatively. The most commonly observed parasites were digenean trematodes, but some nematodes were also recorded. Important differences in parasite prevalence were observed between regions. Further morphological and molecular work will determine potential specificity and prevalence at species level.

Project ParaZoo is funded by the Norwegian Taxonomy Initiative Artsdatabanken.

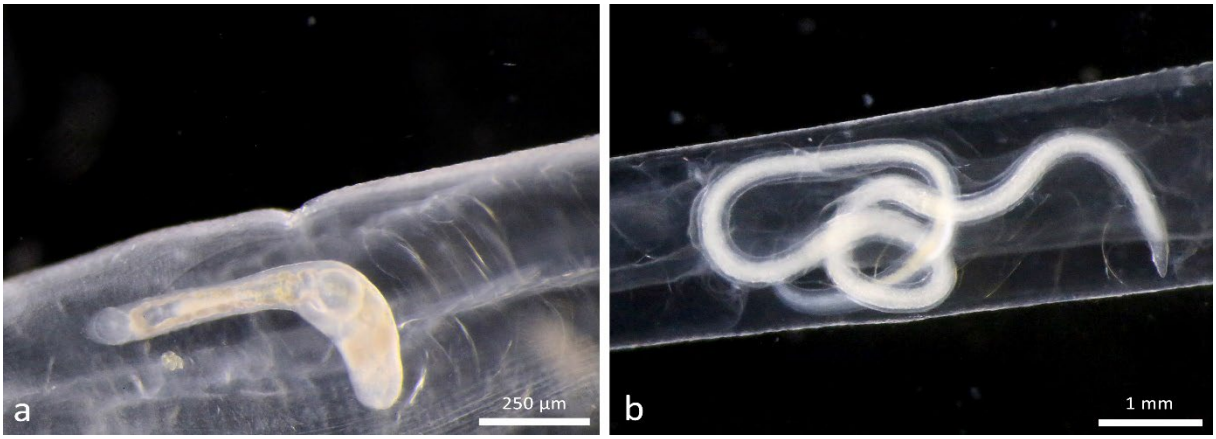

Fig. 5.11 Examples of chaetognath parasites found during the cruise. **a.** Digenean trematode, **b.** nematode.

6 Ship's Meteorological Station

The ship's meteorological station was operational throughout the entire duration of the HE605 expedition, recording wind direction (°), wind speed (m/s), air pressure (hPa), air and water temperature (°C) and humidity.

7 Station List HE605

7.1 Station List

The station list can also be found on PANGAEA:
https://www.pangaea.de/expeditions/events/HE605

Station No.		Date	Gear	Latitude	Longitude	Water Depth	Remarks/Recovery
HEINCKE	AWI	2022		[°N]	[°E]	[m]	
HE605_1-1	KROSS-1	15.8	ROS/CTD	79° 11,755'	011° 47,602'	365	
HE605_1-2	KROSS-1	15.8	GRAB	79° 11,769'	011° 47,868'	362	
HE605_1-3	KROSS-1	15.8	Multi-net	79° 11,152'	011° 47,495'	363	
HE605_1-4	KROSS-1	15.8.	Bongo	79° 11,027'	011° 47,888'	362	
HE605_1-5	KROSS-1	15.8	PELAGIOS	79° 12,230'	011° 48,984'	309	
HE605_2-1	KROSS-2	15.8.	ROS/CTD	79° 07,751'	011° 40,583'	329	
HE605_2-2	KROSS-2	15.8.	GRAB	79° 07,785	011° 40,606'	330	
HE605_2-3	KROSS-2	15.8	Multi-net	79° 07,234'	011° 39,078'	326	
HE605_3-1	KONG-1	15.8	ROS/CTD	78° 58,358'	011° 46,461'	221	
HE605_3-2	KONG-1	15.8	GRAB	78° 58,410'	011° 46,439'	216	
HE605_3-3	KONG-1	15.8	WP3	78° 58,499'	011° 46,020'	188	

HE605_3-4	KONG-1	15.8	Bongo	78° 58,719'	011° 41,419'	326	
HE605_3-5	KONG-1	15.8	Bongo	78° 58,726'	011° 42,470'	312	
HE605_3-6	KONG-1	15.8	Multi-net	78° 58,802'	011° 39,034'	307	
HE605_4-1	KONG-2	16.8	GRAB	78° 55,585'	011° 59,631'	91	
HE605_4-1	KONG-2	16.8	GRAB	78° 55,579'	011° 59,671'	89	
HE605_4-1	KONG-2	16.8	GRAB	78° 55,573'	011° 59,700'	89	
HE605_4-1	KONG-2	16.8	GRAB	78° 55,575'	011° 59,710'	91	
HE605_5-1	KONG-3	16.8	ROS/CTD	78° 56,782'	011° 55,100'	292	
HE605_5-2	KONG-3	16.8	GRAB	78° 56,773'	011° 54,969'	275	
HE605_5-3	KONG-3	16.8	WP3	78° 56,801'	011° 54,940'	284	
HE605_5-4	KONG-3	16.8	WP3	78° 56,794'	011° 54,806'	272	
HE605_5-5	KONG-3	16.8	PELAGIOS	78° 56,775'	011° 54,472'	233	
HE605_5-6	KONG-4	16.8	WP3	78° 56,781'	011° 55,308'	297	
HE605_6-1	KONG-5	16.8	Angling	78° 57,180'	010° 26,362'	81	
HE605_7-1	BIL-1	17.8	ROS/CTD	78° 39,698'	016° 43,890'	192	
HE605_7-2	BIL-1	17.8	GRAB	78° 39,758'	016° 43,930'	192	
HE605_7-3	BIL-1	17.8	WP3	78° 39,858'	016° 43,725'	191	
HE605_7-4	BIL-1	17.8	WP3	78° 39,947'	016° 43,431'	184	
HE605_7-5	BIL-1	17.8	Multi-net	78° 39,198'	016° 40,303'	200	
HE605_8-1	BIL-2	17.8	ROS/CTD	78° 39,555'	016° 40,611'	190	
HE605_8-2	BIL-2	17.8	GRAB	78° 39,550'	016° 40,632'	190	
HE605_8-3	BIL-2	17.8	WP3	78° 39,618'	016° 40,875'	191	
HE605_8-4	BIL-2	17.8	Multi-net	78° 39,102'	016° 38,975'	174	
HE605_9-1	BIL-3	17.8	ROS/CTD	78° 37,562'	016° 33,256'	140	
HE605_9-2	BIL-3	17.8	GRAB	78° 37,571'	016° 33,334'	138	
HE605_9-3(-1)	BIL-3	17.8	WP3	78° 37,755'	016° 33,844'	134	
HE605_9-3(-2)	BIL-3	17.8	WP3	78° 37,590'	016° 33,379'	137	
HE605_9-4	BIL-3	17.8	Multi-net	78° 37,850'	016° 33,526'	147	
HE605_9-5	BIL-3	17.8	OFOS	78° 37,442'	016° 32,716'	147	
HE605_10-1	VMF-1	18.8	ROS/CTD	77° 45,773'	015° 08,472'	105	
HE605_10-2	VMF-1	18.8	GRAB	77° 45,764'	015° 08,389'	105	
HE605_10-3	VMF-1	18.8	GRAB	77° 45,776'	015° 08,292'	104	
HE605_10-4	VMF-1	18.8	GRAB	77° 45,768'	015° 08,267'	104	
HE605_10-5	VMF-1	18.8	WP3	77° 45,771'	015° 08,435'	105	
HE605_10-6	VMF-1	18.8	Multi-net	77° 46,124'	015° 08,240'	104	
HE605_10-7	VMF-1	18.8	Bongo	77° 46,034'	015° 09,567'	104	
HE605_11-1	VMF-2	18.8	ROS/CTD	77° 47,956'	015° 19,809'	104	
HE605_11-2	VMF-2	18.8	GRAB	77° 47,950'	015° 20,284'	105	
HE605_11-3	VMF-2	18.8	WP3	77° 47,936'	015° 20,878'	105	
HE605_11-4	VMF-2	18.8	Multi-net	77° 48,297'	015° 19,126'	103	
HE605_12-1	VMF-3	18.8	ROS/CTD	77° 46,179'	015° 16,764'	101	
HE605_12-2	VMF-3	18.8	GRAB	77° 46,145'	015° 16,904'	100	
HE605_12-3	VMF-3	18.8	WP3	77° 46,127'	015° 17,179'	100	
HE605_12-4	VMF-3	18.8	Multi-net	77° 46,710'	015° 16,601'	106	
HE605_12-5	VMF-3	18.8	OFOS	77° 48,376'	015° 19,359'	103	
HE605_13-1	HORN-1	19.8	ROS/CTD	76° 59,806'	016° 26,708'	125	
HE605_13-2	HORN-1	19.8	GRAB	76° 59,797'	016° 26,880'	126	
HE605_13-3	HORN-1	19.8	GRAB	76° 59,828'	016° 26,786'	125	
HE605_13-4	HORN-1	19.8	GRAB	76° 59,825'	016° 26,776'	125	
HE605_13-5	HORN-1	19.8	WP3	76° 59,749'	016° 26,942'	124	
HE605_13-6	HORN-1	19.8	Multi-net	76° 59,664'	016° 25,976'	127	
HE605_13-7	HORN-1	19.8	Bongo	76° 59,678'	016° 26,878'	124	
HE605_13-8	HORN-1	19.8	OFOS	76° 59,838'	016° 27,057'	125	
HE605_14-1	HORN-2	19.8	ROS/CTD	76° 59,519'	016° 00,681'	107	
HE605_14-2	HORN-2	19.8	GRAB	76° 59,499'	016° 00,600'	106	
HE605_14-3	HORN-2	19.8	Multi-net	76° 59,332'	015° 59,994'	113	
HE605_15-1	HORN-3	19.8	ROS/CTD	76° 57,742'	015° 49,667'	223	
HE605_15-2	HORN-3	19.8	GRAB	76° 57,757'	015° 49,603'	222	
HE605_15-3	HORN-3	19.8	WP3	76° 57,730'	015° 49,557'	223	
HE605_15-4	HORN-3	19.8	Multi-net	76° 58,063'	015° 50,709'	211	
HE605_16-1	HORN-4	19.8	PELAGIOS	76° 59,266'	015° 49,480'	200	
HE605_17-1	SPITSB-1	20.8	Angling	75° 14,554'	018° 34,672'	24	
HE605_18-1	BAR-1	21.8	ROS/CTD	72° 16,771'	024° 26,181'	268	
HE605_18-2	BAR-1	21.8	GRAB	72° 16,749'	024° 26,258'	267	

HE605_18-3	BAR-1	21.8	WP3	72° 16,795'	024° 26,123'	250	
HE605_18-4	BAR-1	21.8	Multi-net	72° 17,390'	024° 26,728'	266	
HE605_18-5	BAR-1	21.8	PELAGIOS	72° 17,892'	024° 27,466'	268	
HE605_18-6	BAR-1	21.8	Bongo	72° 19,395'	024° 29,092'	266	
HE605_19-2	BAR-2	21.8	ROS/CTD	71° 48,735'	025° 34,401'	282	
HE605_19-3	BAR-2	21.8	GRAB	71° 48,761'	025° 34,394'	280	
HE605_19-4	BAR-2	21.8	Multi-net	71° 49,013'	025° 36,159'	286	
HE605_20-1	BAR-3	21.8	ROS/CTD	71° 41,652'	026° 12,151'	326	
HE605_20-2	BAR-3	21.8	GRAB	71° 41,635'	026° 12,171'	325	
HE605_20-3	BAR-3	21.8	WP3	71° 41,626'	026° 12,197'	326	
HE605_20-4	BAR-3	21.8	Multi-net	71° 41,462'	026° 14,318'	327	
HE605_20-5	BAR-3	21.8	Bongo	71° 41,184'	026° 18,314'	335	
HE605_21-1	POR-1	22.8	ROS/CTD	70° 31,774'	025° 39,012'	152	
HE605_21-2	POR-1	22.8	ROS/CTD	70° 31,761'	025° 39,057'	150	
HE605_21-3	POR-1	22.8	ROS/CTD	70° 31,772'	025° 39,081'	150	
HE605_21-4	POR-1	22.8	ROS/CTD	70° 31,746'	025° 39,154'	148	
HE605_21-5	POR-1	22.8	ROS/CTD	70° 31,731'	025° 38,949'	152	
HE605_21-6	POR-1	22.8	ROS/CTD	70° 31,714'	025° 39,067'	148	
HE605_21-7	POR-1	22.8	GRAB	70° 31,680'	025° 39,192'	146	
HE605_21-8	POR-1	22.8	WP3	70° 31,707'	025° 39,070'	148	
HE605_21-9	POR-1	22.8	WP3	70° 31,750'	025° 39,454'	147	
HE605_21-10	POR-1	22.8	Multi-net	70° 31,966'	025° 39,657'	158	
HE605_21-11	POR-1	22.8	Bongo	70° 31,954'	025° 39,162'	168	
HE605_21-12	POR-1	22.8	BlueROV2	70° 31,865'	025° 39,052'	158	Zodiac for ROV deployment
HE605_22-1	POR-2	22.8	angling	70° 24,958'	025° 19,783'	34	
HE605_23-1	POR-3	24.8	ROS/CTD	70° 05,294'	025° 06,593'	78	
HE605_23-2	POR-3	24.8	GRAB	70° 05,270'	025° 06,650'	77	
HE605_23-3	POR-3	24.8	GRAB	70° 05,260'	025° 06,615'	75	
HE605_23-4	POR-3	24.8	GRAB	70° 05,258'	025° 06,560'	75	
HE605_23-5	POR-3	24.8	GRAB	70° 05,266'	025° 06,526'	75	
HE605_23-6	POR-3	24.8	GRAB	70° 05,275'	025° 06,522'	75	
HE605_23-7	POR-3	24.8	WP3	70° 05,279'	025° 06,628'	77	
HE605_23-8	POR-3	24.8	Multi-net	70° 05,158'	025° 06,263'	67	
HE605_23-9	POR-3	24.8	Bongo	70° 05,457'	025° 07,098'	89	
HE605_23-10	POR-3	24.8	WP3	70° 05,442'	025° 07,316'	84	
HE605_23-11	POR-3	24.8	WP3	70° 05,486'	025° 07,332'	87	
HE605_23-12	POR-3	24.8	OFOS	70° 05,294'	025° 06,545'	77	
HE605_23-13	POR-3	24.8	PELAGIOS	70° 06,501'	025° 09,047'	104	
HE605_24-1	POR-4	25.8	ROS/CTD	70° 18,584'	025° 18,021'	87	
HE605_24-2	POR-4	25.8	GRAB	70° 18,593'	025° 18,031'	85	
HE605_24-3	POR-4	25.8	GRAB	70° 18,586'	025° 18,025'	87	
HE605_24-4	POR-4	25.8	GRAB	70° 18,598'	025° 17,999'	84	
HE605_24-5	POR-4	25.8	GRAB	70° 18,565'	025° 18,006'	88	
HE605_24-6	POR-4	25.8	GRAB	70° 18,521'	025° 18,022'	89	
HE605_24-7	POR-4	25.8	GRAB	70° 18,503'	025° 18,084'	88	
HE605_24-8	POR-4	25.8	GRAB	70° 18,528'	025° 18,072'	88	
HE605_24-9	POR-4	25.8	WP3	70° 18,570'	025° 18,041'	87	
HE605_24-10	POR-4	25.8	Multi-net	70° 18,693'	025° 18,109'	81	
HE605_24-11	POR-4	25.8	Bongo	70° 18,976'	025° 18,581'	96	
HE605_24-12	POR-4	25.8	WP3	70° 19,061'	025° 18,719'	97	
HE605_24-13	POR-4	25.8	OFOS	70° 19,126'	025° 18,271'	96	
HE605_24-14	POR-4	25.8	PELAGIOS	70° 19,865'	025° 19,635'	84	
HE605_25-1	POR-5	25.8	angling	70° 31,682'	025° 22,824'	45	
HE605_26-1	POR-6	26-1	ROS/CTD	70° 53,197'	026° 03,939'	194	
HE605_26-2	POR-6	26.8	GRAB	70° 53,246'	026° 04,099'	193	
HE605_26-3	POR-6	26.8	GRAB	70° 53,235'	026° 04,016'	193	
HE605_26-4	POR-6	26.8	GRAB	70° 53,226'	026° 03,972'	193	
HE605_26-5	POR-6	26.8	GRAB	70° 53,222'	026° 03,941'	193	
HE605_26-6	POR-6	26.8	GRAB	70° 53,202'	026° 03,888'	193	
HE605_26-7	POR-6	26.8	GRAB	70° 53,184'	026° 03,844'	194	
HE605_26-8	POR-6	26.8	WP3	70° 53,116'	026° 03,812'	194	
HE605_26-9	POR-6	26.8	WP3	70° 52,985'	026° 03,761'	194	
HE605_26-10	POR-6	26.8	Multi-net	70° 53,186'	026° 03,807'	194	
HE605_26-11	POR-6	26.8	Bongo	70° 53,882'	026° 04,217'	194	

HE605_26-12	POR-6	26.8	OFOS	70° 54,364'	026° 04,366'	194	
HE605_27-1	POR-7	27-1	ROS/CTD	71° 05,466'	026° 19,723'	165	
HE605_27-2	POR-7	26.8	GRAB	71° 05,448'	026° 19,775'	174	Failed to take sediment
HE605_27-2	POR-7	26.8	GRAB	71° 05,450'	026° 19,766'	171	Failed to take sediment
HE605_27-2	POR-7	26.8	GRAB	71° 05,451'	026° 19,756'	172	Failed to take sediment
HE605_27-3	POR-7	26.8	WP3	71° 05,464'	026° 19,743'	164	
HE605_27-4	POR-7	26.8	Multi-net	71° 05,732'	026° 19,838'	96	
HE605_27-5	POR-7	26.8	WP3	71° 05,467'	026° 19,731'	163	
HE605_27-6	POR-7	26.8	Bongo	71° 06,245'	026° 19,716'	148	
HE605_27-7	POR-7	26.8	Bongo	71° 06,798'	026° 19,495'	199	
HE605_28-1	POR-8	28-1	angling	71° 01,639'	026° 15,316'	120	
HE605_29_1	BLC-1	29-1	ROS/CTD	69° 30,355'	015° 45,680'	631	
HE605_29_2	BLC-1	29-2	ROS/CTD	69° 30,356'	015° 45,653'	637	
HE605_29-3	BLC-1	29.8	GRAB	69° 30,351'	015° 45,482'	660	Failed to take sediment
HE605_29-4	BLC-1	29.8	GRAB	69° 30,356'	015° 45,468'	664	Failed to take sediment
HE605_29-5	BLC-1	29.8	WP3	69° 30,352'	015° 45,455'	668	
HE605_29-6	BLC-1	29.8	Multi-net	69° 30,133'	015° 45,663'	601	
HE605_29-7	BLC-1	29.8	Bongo	69° 30,675'	015° 46,860'	532	
HE605_30_1	BLC-2	30-1	ROS/CTD	69° 28,008'	015° 39,007'	1112	
HE605_30_2	BLC-2	30-2	ROS/CTD	69° 28,029'	015° 39,011'	1279	
HE605_30-3	BLC-2	29.08	GRAB	69° 28,054'	015° 39,007	1290	
HE605_30-4	BLC-2	29.8	WP3	69° 28,016'	015° 39,068'	1281	
HE605_30-5	BLC-2	29.8	Multi-net	69° 27,935'	015° 39,266'	1222	
HE605_31-1	BLC-3	31-1	ROS/CTD	69° 29,737'	015° 47,560'	314	Water sampling failed
HE605_31-3	BLC-3	30.8	WP3	69° 29,744'	015° 47,483'	323	
HE605_31-4	BLC-3	30.8	WP3	69° 29,726'	015° 47,528'	316	
HE605_31-5	BLC-3	30.8	WP3	69° 29,713'	015° 47,487'	321	
HE605_31-6	BLC-3	30.8	Multi-Net	69° 29,654'	015° 47,345'	337	
HE605_31-7	BLC-3	30.8	Bongo	69° 29,025'	015° 44,762'	690	

8 Data and Sample Storage and Availability

Evaluation, analysis and publication of the research data from this cruise are still ongoing. Hence, the datasets currently available are limited (Table 8.1), but will be produced and submitted to public databases over the next three years.

Zooplankton samples will be archived and stored at the AWI and the University Museum of Bergen. DNA extracts of GZP and other plankton, and remaining DNA extracts from eDNA filters and sediment will be stored at -80°C in the AWI and Uni Bergen for up to ten years after publication of the results (according to the DFG guidelines for good scientific practice). A voucher collection of ethanol-preserved jelly specimens, linked to their DNA extracts by unique sample identifiers, will be kept in a repository at the AWI and at Uni Bergen. Geo-referenced datasets including species inventories, distribution records, video footages (snapshots of video observations) and abundance data of macrozooplankton from net catches will be submitted to the World Data Center PANGAEA Data Publisher for Earth & Environmental Science (https://www.pangaea.de) as soon as the data are available (within two years after the cruise at the latest), possibly with an embargo period until publications have been finalized. By default, the CC-BY license will be applied. Biogeographic datasets will also feed other databases (e.g., OBIS, GBIF).

Molecular data will be archived, published and disseminated within one of the repositories of the International Nucleotide Sequence Data Collaboration (INSDC, www.insdc.org) comprising of EMBL-EBI/ENA, GenBank and DDBJ. Results on eDNA metabarcoding analyses will be published in peer-reviewed journals within three years after the cruise. Any other data will be submitted to an appropriate long-term archive that provides unique and stable identifiers for the datasets and allows open online access to the data.

In all publications, based on this cruise, the **Grant No. AWI_HE605_00** will be quoted.

Table 8.1 Overview of data availability

Type	Database	Availability and Contact
Master track HE605	PANGAEA	https://doi.org/10.1594/PANGAEA.950690
Master tracks HE605, alternative resolutions	PANGAEA	https://doi.org/10.1594/PANGAEA.950689
Event list HE605	PANGAEA	https://www.pangaea.de/expeditions/events/HE605
Physical Oceanography, raw data CTD	PANGAEA	To be added on PANGAEA soon (2023), Charlotte.Havermans@awi.de
GZP distributions and diversity	PANGAEA	To be added on PANGAEA (2023/24, embargo till 2025), Charlotte.Havermans@awi.de; Aino.Hosia@uib.no; Joan.Soto@uib.no
GZP genetic barcodes	BOLD/ GenBank	To be added on BOLD/GenBank (2023/24, embargo till 2025), Charlotte.Havermans@awi.de; Aino.Hosia@uib.no; Joan.Soto@uib.no; Luis.Martell@uib.no
Other ecological information and ongoing studies	(various)	Various ongoing studies, publications planned for the next three years Main contact: Charlotte.Havermans@awi.de

9 Acknowledgements

We are very grateful to R/V Heincke's Master Haye Diecks and the ship's crew for their skillful support and the excellent working atmosphere on board. We also thank the AWI logistics and ship's coordination for their support.
The HE605 expedition has been conducted in the framework of the **Helmholtz Young Investigator Group "ARJEL – Arctic Jellies"** with the project number VH-NG-1400, funded by the Helmholtz Society and the Alfred Wegener Institute Helmholtz Centre for Polar and Marine Research. It was further supported by the Helmholtz Research Programme "Changing Earth – Sustaining our Future" Topic 6, Subtopics 6.1 and 6.2.
C. Havermans, A. Eschbach, A. Dischereit, J. Throm, I. Rathnayake and N. Steiner were funded through the Helmholtz Young Investigator Group "ARJEL – Arctic Jellies".
J. Soto-Angel was funded by the POLE2POLE project of the Marie Skłodowska-Curie Actions MSCA programme, Horizon2020, European Commission (Grant code: 101031845). H. Hampe and V. Stenvers were supported by the Emmy Noether Junior Research Group of the Deutsche Forschungsgemeinschaft (DFG) under grant HO 5569/2-1 to PI H.J. Hoving. Additional projects contributing to this expedition are: *ParaZoo*, funded by the Norwegian Taxonomy Initiative Artsdatabanken, and the project *iAtlantic*, funded by the European Union's Horizon 2020 Research and Innovation Programme (Grant code: 818123).

10 References

Allcock, A.L., Griffiths, H.J., 2014. Bipolarity. In: De Broyer, C., Koubbi, P., Griffiths, H.J., Raymond, B., d'Udekem d'Acoz, C., Van de Putte, A., Danis, B., Grant, S., Gutt, J., Held, C., Hosie, G., Huettmann, F., Post, A., Ropert-Coudert, Y. (Eds.), Biogeographic Atlas of the Southern Ocean. Scientific Committee on Antarctic Research, Cambridge, 431–436.

Arnkvaern, G., Daase, M., Eiane, K., 2005. Dynamics of coexisting *Calanus finmarchicus*, *Calanus glacialis* and *Calanus hyperboreus* populations in a high-Arctic fjord. Polar Biology, 28, 528–538.

Bae, S., Kim, H., Nam, S.I., Choi, K.H., Kim, T.W., Yun, S.T., Kim, H.S., Kim, T.H., Han, D., Ko, Y.H., Kim, J.H., Lim, Y.K., Park, J.M. (2022). The composition and abundance of

phytoplankton after spring bloom in the Arctic Svalbard fjords. Estuarine, Coastal and Shelf Science, 275,107970.

Blaszczyk, M., Jacek, J. A., Leszek, K., 2013. Fluctuations of tidewater glaciers in Hornsund Fjord (Southern Svalbard) since the beginning of the 20th century. Polish Polar Research, 34(4), 327–352.

Blindheim, J., 1985. Ecological features of the Norwegian Sea. In: Rey L, Alexander V, editors. Proceedings of the Sixth Conference of the Comité Arctique International, Fairbanks, Alaska, 13–15 May, p 366–401.

Botterell, L.R., Beaumont, N., Dorrington, T., Steinke, M., Thompson, R.C., Lindeque, P.K., 2019. Bioavailability and effects of microplastics on marine zooplankton. Environmental Pollution, 245, 98–110.

Buchholz, F., Buchholz, C., Węsławski, J.M., 2010. Ten years after: Krill as indicator of changes in the macro-zooplankton communities of two Arctic fjords. Polar Biology, 33, 101–113.

Carmack, E., Wassmann, P., 2006. Food webs and physical-biological coupling on pan-Arctic shelves: unifying concepts and comprehensive perspectives. Progress in Oceanography, 71, 446–477.

Christiansen, B., Denda, A., Christiansen, S., 2020. Potential effects of deep seabed mining on pelagic and benthopelagic biota. Marine Policy, 114, 103442.

Christiansen, J.S., Fevolden, S.-E., 2000. The polar cod of Porsangerfjorden, Norway; revisited. Sarsia, 85, 189–193.

Cisek, M., Makuch, P., Petelski, T., 2017. Comparison of meteorological conditions in Svalbard fjords: Hornsund and Kongsfjorden. *Oceanologia*, 59, 413–421.

Cottier, F., Tverberg, V., Inall, M., Svendsen, H., Nilsen, F., & Griffiths, C., 2005. Water mass modification in an Arctic fjord through cross-shelf exchange: The seasonal hydrography of Kongsfjorden, Svalbard. Journal of Geophysical Research: Oceans, 110(C12005), 1–18.

Cottier, F. R., Nilsen, F., Skogseth, R., Tverberg, V., Skardhamar, J., & Svendsen, H., 2010. Arctic fjords: A review of the oceanographic environment and dominant physical processes. Geological Society Special Publication, 344, 35–50.

Crame, J.A., 1993. Bipolar molluscs and their evolutionary implications. Journal of Biogeography, 20, 145–161.

Daponte, M.C., Gil de Pertierra, A.A., Palmieri, M.A., Ostrowski de Nuñez, M., 2008. Monthly occurrence of parasites of the chaetognath *Sagitta friderici* off Mar del Plata, Argentina. Journal of Plankton Research, 30, 567–576.

De Jonge, D., Merten, V., Bayer, T., Puebla, O., Reusch, T.B.H., Hoving, H.J.T., 2021. Novel metabarcoding primer pair for environmental DNA analysis of Cephalopoda (Mollusca) targeting the nuclear 18S rRNA region. Royal Society Open Science, 8, 201388.

Descôteaux, R., Ershova, E., Wangensteen, O.S., Praebel, K., Renaud, P.E., Cottier, F., Bluhm, B.A. (2021). Meroplankton diversity, seasonality and life-history traits across the Barents Sea Polar Front revealed by high-throughput DNA barcoding. Frontiers in Marine Science 8, 677732.

Drazen, J. C., Smith, C. R., Gjerde, K. M., Haddock, S. H. D., Carter, G. S., Choy, C. A., Clark, M. R., Dutrieux, P., Goetze, E., Hauton, C., Hatta, M., Koslow, J. A., Leitner, A. B., Pacini, A., Perelman, J. N., Peacock, T., Sutton, T. T., Watling, L., Yamamoto, H., 2020. Opinion: Midwater ecosystems must be considered when evaluating environmental risks of deep-sea mining. Proceedings of the National Academy of Sciences, 117(30), 17455.

Dunlop, K.M., Jones, D.O.B., Sweetman, A.K., 2017. Direct evidence of an efficient energy transfer pathway from jellyfish carcasses to a commercially important deep-water species. Scientific Reports, 7, 17455.

Eilertsen, H.C., Frantzen, S., 2007. Phytoplankton from two sub-Arctic fjords in northern Norway 2002-2004: I. Seasonal variations in chlorophyll a and bloom dynamics. Marine Biol Research, 3, 319-332.

Fer, I., Widell, K., 2007. Early spring turbulent mixing in an ice-covered Arctic fjord during transition to melting. Continental Shelf Research, 27(15), 1980–1999.

Galloway, T.S., Cole, M., Lewis, C., 2017. Interactions of microplastic debris throughout the marine ecosystem. Nature Ecology and Evolution, 1, 0116.

Geoffroy, M., Berge, J., Majaneva, S., Johnsen, G., Langbehn, T.J., Cottier, F., Mogstad, A.A., Zolich, A., Last, K., 2018. Increased occurrence of the jellyfish *Periphylla periphylla* in the European high Arctic. Polar Biology, 41, 2615–2619.

Günther, B., Fromentin, J., Metral, L., Arnaud-Haond, S., 2021. Metabarcoding confirms the opportunistic foraging behaviour of Atlantic bluefin tuna and reveals the importance of gelatinous prey. PeerJ, 9, e11757.

Havermans, C., Dischereit, A., Pantiukhin, D., Friedrich, M., Murray, A., 2022. Environmental DNA in an ocean of change: Status, challenges and prospects. Arquivos de Ciências do Mar, 55, 298–337.

Havermans, C., Smetacek, V., 2018. Bottom-up and top-down triggers of diversification: A new look at the evolutionary ecology of scavenging amphipods in the deep sea. Progress in Oceanography, 164, 37–51.

Hop, H., Wold, A., Vihtakari, M., Daase, M., Kwasniewski, S., Gluchowska, M., Lischka, S., Buchholz, F., Falk-Petersen, S., 2019. Zooplankton in Kongsfjorden (1996-2016) in relation to climate change. In: Hop, H., Wiencke, C. (eds.) The ecosystem of Kongsfjorden, Svalbard. Advances in Polar Ecology, vol. 2, Springer, Cham.

Hoving, H.J.T., Christiansen, S., Fabrizius, E., Hauss, H., Kiko, R., Linke, P., Neitzel, P., Piatkowski, U., Körtzinger, A., 2019. The Pelagic In situ Observation System (PELAGIOS) to reveal biodiversity, behavior and ecology of elusive oceanic fauna. Ocean Science Discussions, 15(5), 1327–1340.

Hoving, H.J.T., Haddock, S.H.D., 2017. The deep-sea giant octopus *Haliphron atlanticus* forages on gelatinous zooplankton. Scientific Reports, 7, 44952.

Hoving, H.J.T., Zeidberg, L, Benfield, M., Bush, S., Robison, B., Vecchione, M. (2013). First in situ observations of the deep-sea squid *Grimalditeuthis bonplandi* reveals unique use of tentacles. Proceedings of the Royal Society B: Biological Sciences, 280, 1769.

Jakobsen, T., Ozhigin, V.K., 2011. The Barents Sea: Ecosystem, Resources, Management: Half a century of Russian-Norwegian cooperation. Trondheim, Tapir Academic Press.

Jensen, M.R., Sigsgaard, E.E., de Paula Avila, M., Agersnap, S., Brenner-Larsen, W., Sengupta, M.E., Xing, Y., Krag, M.A., Knudsen, S.W., Carl, H., Møller, P.R., Thomsen, P.F., 2022. Short-term temporal variation of coastal marine eDNA. Environmental DNA, 4(4), 747-762.

Källgren, E.K., Pedersen, T., Nilssen, E.M., 2015. Food resource partitioning between three sympatric fish species in Porsangerfjord, Norway. Polar Biology, 38, 583–589.

Laberg, J.S., Vorren, T.O., Knutsen, S.M., 1999. The Lofoten Contourite off Norway. Marine Geology, 159, 1–6.

Laberg, J.S., Guidard, S., Mienert, J., Vorren, T.O., Haflidason, H., Nygård, A., 2007. Morphology and morphogenesis of a high-latitude canyon: The Andøya Canyon, Norwegian Sea. Marine Geology, 246, 68–85.

Lebrato, M., Mendes, P.J., Steinberg, D.K., Cartes, J.E., Jones, B.M., Birsa, L., Benavides, R., Oschlies, A., 2013. Jelly biomass sinking speed reveals a fast carbon export mechanism. Limnology and Oceanography, 58, 1113–1122.

Leray, M., Yang, J.Y., Meyer, C.P., Mills S.C., Agudelo N., Ranwez, V., Boehm, J.T., Machida R.J., 2013. A new versatile primer set targeting a short fragment of the mitochondrial COI region for metabarcoding metazoan diversity; application for characterizing coral reef fish gut contents. Frontiers in Zoology, 10, 34.

Lind, S., Ingvaldsen, R.B., 2012. Variability and impacts of Atlantic Water entering the Barents Sea from the north. Deep Sea Research Part I Oceanography Research Papers, 62, 70–88.

Magerud, J., Svendsen, J.I., 2018. The Holocene Thermal Maximum around Svalbard, Arctic North Atlantic; molluscs show early and exceptional warmth. The Holocene 28(1), 65–83.

Neukermans, G., Oziel, L., Babin, M., 2018. Increased intrusion of warming Atlantic water leads to rapid expansion of temperate phytoplankton in the Arctic. Global Change Biology 24(6), 2545–2553.

Nilsen, F., Cottier, F., Skogseth, R., Mattsson, S. 2008. Fjord-shelf exchanges controlled by ice and brine production: the interannual variation of Atlantic Water in Isfjorden, Svalbard

Continental Shelf Research, 28, 1838–1853.

Nilsen, F., Skogseth, R., Vaardal-Lunde, J., Inall, M., 2016. A simple shelf circulation model: Intrusion of Atlantic Water on the West Spitsbergen Shelf. Journal of Physical Oceanography, 46(4), 1209–1230.

Øresland, V., 1986. Parasites of the chaetognath *Sagitta setosa* in the western English Channel. Marine Biology, 92, 87–91.

Oziel, L., Sirven, J., Gascard, J.-C., 2016. The Barents Sea frontal zones and water masses variability (1980-2011). Ocean Science, 12, 169–184.

Payne, C.M., Roesler, C.S., 2019. Characterizing the influence of Atlantic water intrusion on water mass formation and phytoplankton distribution in Kongsfjorden, Svalbard. Continental Shelf Research, 191, 104005.

Pearre, S., 1979. Niche modification in Chaetognatha infected with larval trematodes (Digenea). Int. Rev. Gesamten. Hydrobiol. Hydrogr. 64, 193–206.

Promińska, A., Cisek, M., & Walczowski, W., 2017. Kongsfjorden and Hornsund hydrography–comparative study based on a multiyear survey in fjords of West Spitsbergen. Oceanologia, 59, 397–412.

Questel, J.M., Hopcroft, R.R., DeHart, H.M., Smoot, C.A., Kosobokova, K.N., 2021. Metabarcoding of zooplankton diversity within the Chukchi Borderland, Arctic Ocean: improved resolution from multi-gene markers and region-specific DNA databases. Marine Biodiversity, 51, 1–19.

Rathnayake, I., 2022. Diet analysis of two hyperiid amphipods in the southern Benguela Upwelling System using DNA metabarcoding, MSc thesis, University of Bremen, 89 pp.

Renaud, P.E., Sejr, M.K., Bluhm, B.A., Sirenko, B., Ellingsen, I.H., 2015. The future of Arctic benthos: expansion, invasion, and biodiversity. Progress in Oceanography, 139, 244–257.

Rødland, E.S., Bjørge, A., 2015. Residency and abundance of sperm whales (*Physeter macrocephalus*) in the Bleik Canyon, Norway. Marine Biology Research, 11(9).

Skarðhamar, J., Svendsen, H., 2010. Short-term hydrographic variability in a stratified Arctic fjord. Geological Society Special Publication, 344: 51–60.

Skjoldal, H.R., 2004. The Norwegian Sea Ecosystem. Trondheim: Tapir Academic Press. 559pp.

Steer, M., Cole, M., Thompson, R.C., Lindeque, P.K., 2017. Microplastic ingestion in fish larvae in the western English Channel. Environmental Pollution, 226, 250-259.

Stepanjants, S.D., Cortese, G., Kruglikova, S.B., Bjørklund, K.R., 2006. A review of bipolarity concepts: history and examples from Radiolaria and Medusozoa (Cnidaria). Marine Biology Research, 2, 200–241.

Sternal, B., Szczuciski, W., Forwick, M., Zajaczkowski, M., Lorenc, S., Przytarska J., 2014. Postglacial variability in near-bottom current speed on the continental shelf off south-west Spitsbergen. Journal of Quaternary Science, 29(8), 767–777.

Svendsen, H, 1991. Preliminary results from a hydrophysical investigation of Porsangerfjord, Altafjord and adjacent coastal waters, June-August 1990. Report of the Geophysical Institute, University of Bergen, Norway, pp. 1–28.

Svendsen, H., Beszczynska-Møller, A., Hagen, J.O., Lefauconnier, B., Tverberg, V., Gerland, S., Ørbaek, J.B., Bischof, K., Papucci, C., Zajaczkowski, M., Azzolini, R., Bruland, O., Wiencke, C., Winther, J.-G., Dallmann, W., 2002. The physical environment of

Kongsfjorden-Krossfjorden, an Arctic fjord system in Svalbard. Polar Research 21, 133–166.

Svendsen, Y.S., 1990. Hosts of third stage larvae of *Hysterothylacium* sp. (Nematoda, Anisakidae) in zooplankton from outer Oslofjord, Norway. Sarsia, 75(2), 161–167.

Swerpel, S., 1985. The Hornsund Fjord: Water Masses. Polish Polar Research, 6(4), 475–496.

Thompson, R.C., Olsen, Y., Mitchell, R.P., Davis, A., Rowland, S.J., John, A.W.G., McGonigle, D., Russell, A.E., 2004. Lost at sea: where is all the plastic? Science, 304, 838.

van de Poll, W.H., Kulk, G., Rozema, P.D., Brussaard, C.P.D., Visser, R.J.W., Buma, A.G.J., 2018. Contrasting glacial meltwater effects on post-bloom phytoplankton on temporal and spatial scales in Kongsfjorden, Spitsbergen. Elementa Science of the Anthropocene, 6, 50.

van der Grient, J. M. A., & Drazen, J. C., 2022. Evaluating deep-sea communities' susceptibility to mining plumes using shallow-water data. Science of The Total Environment, 158162.

Walkusz, W., Storemark, K., Skau, T., Gannefors, C., Lundberg, M., 2003. Zooplankton community structure; a comparison of fjords, open water and ice stations in the Svalbard area. Polish Polar Research, 24, 149–165.

Washburn, T. W., Turner, P. J., Durden, J. M., Jones, D. O. B., Weaver, P., Van Dover, C. L. 2019. Ecological risk assessment for deep-sea mining. Ocean & Coastal Management, 176, 24–39.

Wassmann, P., Svendsen, H., Keck, A., Reigstad, M., 1996. Selected aspects of the physical oceanography and particle fluxes in fjords of northern Norway. Journal of Marine Systems, 8, 53-71.

Węsławski, J.M., Koszteyn, J., Zajaczkowski, M., Wiktor, J., Kwaśniewski, S., 1995.

Fresh water in Svalbard fjord ecosystems. In: Skjoldal, R., Hopkins, C., Erikstad, K.E., Leinaa, H.P. (Eds.), Ecology of Fjords and Coastal Waters, 229–241.

Yamamoto, J., Hirose, M., Ohtani, T., Sugimoto, K., Hirase, K., Shimamoto, N., Shimura, T., Honda, N., Fujimori, Y., Mukai, T., 2008. Transportation of organic matter to the sea floor by carrion falls of the giant jellyfish *Nemopilema nomurai* in the Sea of Japan. Marine Biology, 153, 311–317.

11 Abbreviations

BONGO: Bongo nets

CTD: Conductivity, Temperature, Depth

GZP: gelatinous zooplankton

ROV: Remotely Operated Vehicle

12 Appendices

12.1 Selected Pictures of Samples

Fig. 12.1.1 Examples of benthic animals retrieved from the Van Veen Grab samples. Different taxa such as echinoderms, bivalves, and polychaetes were sampled and will be barcoded to enhance reference libraries for eDNA analyses.

12.2 Selected Pictures of Shipboard Operations

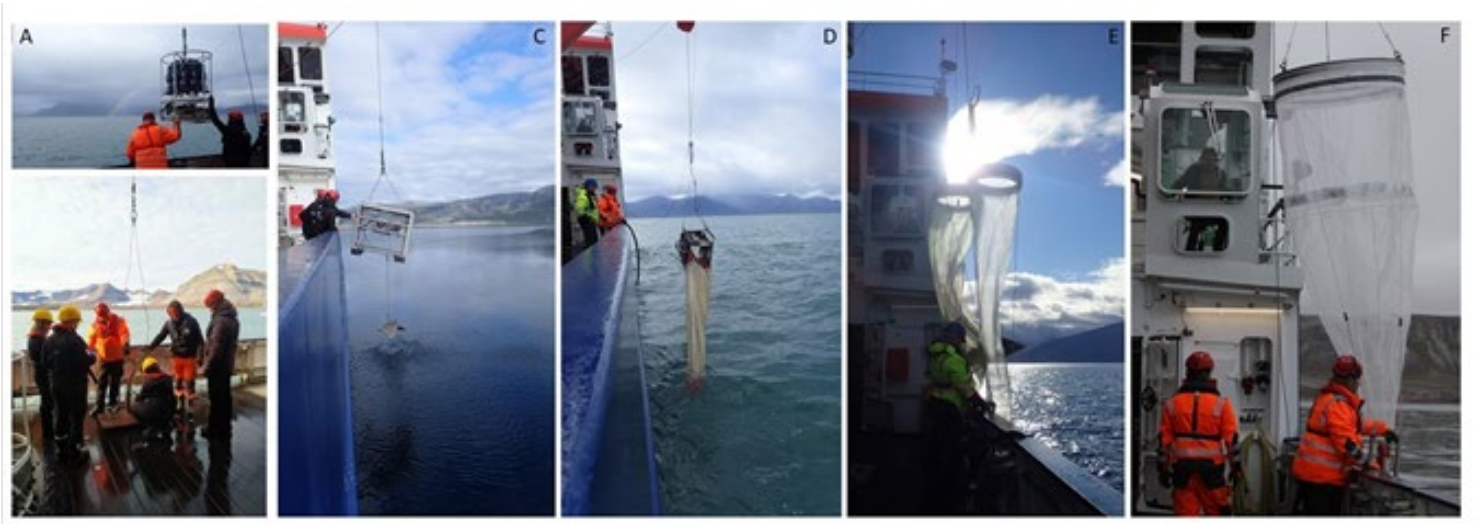

Fig. 12.2.1 A. CTD; B. Van Veen Grab; C. PELAGIOS; D. Multi-net; E. Bongo net; F. WP3 net.